

Food & Function

Linking the chemistry and physics of food with health and nutrition

Accepted Manuscript

This article can be cited before page numbers have been issued, to do this please use: N. Batra, P. R. Rout and P. Dey, *Food Funct.*, 2026, DOI: 10.1039/D5FO04976H.



This is an Accepted Manuscript, which has been through the Royal Society of Chemistry peer review process and has been accepted for publication.

Accepted Manuscripts are published online shortly after acceptance, before technical editing, formatting and proof reading. Using this free service, authors can make their results available to the community, in citable form, before we publish the edited article. We will replace this Accepted Manuscript with the edited and formatted Advance Article as soon as it is available.

You can find more information about Accepted Manuscripts in the [Information for Authors](#).

Please note that technical editing may introduce minor changes to the text and/or graphics, which may alter content. The journal's standard [Terms & Conditions](#) and the [Ethical guidelines](#) still apply. In no event shall the Royal Society of Chemistry be held responsible for any errors or omissions in this Accepted Manuscript or any consequences arising from the use of any information it contains.

1 **Modulation and adaptation of gut microbial metabolic functions under**
2 **probiotic and postbiotic treatment using a novel *in vitro* anaerobic**
3 **pseudo-colon system**

4
5 Nehal Batra¹, Prangya Ranjan Rout², Priyankar Dey^{1*}

6
7 ¹ Department of Biotechnology, Thapar Institute of Engineering and Technology,
8 Patiala 147004, Punjab, India

9 ² Department of Biotechnology, Dr. B.R. Ambedkar National Institute of Technology,
10 Jalandhar, India

11
12 *Corresponding author

13 Email: priyankar.dey@thapar.edu; priyankardey28@gmail.com

14 Mob: +91-9064275660



15 **Abstract**

View Article Online
DOI: 10.1039/D5FO04976H

16 Probiotics and postbiotics compounds found in food influence gut microbiota to attenuate
17 chronic metabolic diseases; however, the underlying mechanisms are not yet fully understood. This
18 study employed a customized *in vitro* anaerobic pseudo-colon system (AMMR) to evaluate the
19 impacts of *Lactiplantibacillus plantarum* (probiotic) and butyrate (postbiotic) on gut microbial
20 composition and functionality, using human fecal samples. Metagenomic (16S rRNA) profiling and
21 untargeted metabolomic (GC-MS) analysis were conducted after 48-h treatments. The results
22 showed that butyrate supplementation markedly enhanced microbial diversity, inhibited opportunistic
23 pathobionts (e.g., *Enterococcus*, *Klebsiella*), and selectively enriched butyrate producers (e.g.,
24 *Lachnoclostridium*), while diminishing the Firmicutes:Bacteroidetes ratio. It increased indole levels
25 metabolically and redirected pathways towards amino acid synthesis and energy metabolism, while
26 suppressing fatty acid formation. Contrarily, *L. plantarum* exhibited modest alterations in microbial
27 diversity while enhancing *Bacteroides* and *Klebsiella*, and preserving elevated *Enterococcus* levels.
28 It elevated saturated fatty acids (octanoic/capric acid) and enhanced amino acid catabolic pathways
29 (valine/leucine) and redox regulators (taurine metabolism). Correlation analysis revealed that
30 butyrate was associated with fiber-degrading microbes, whereas *L. plantarum* was associated with
31 lactic acid bacteria, suggesting distinct ecological niches and interaction patterns. These findings
32 collectively indicate that butyrate and *L. plantarum* elicit complementary microbial alterations, i.e.,
33 butyrate directly transforms microbial structure and metabolism towards an anti-inflammatory
34 phenotype, while *L. plantarum* largely influences via metabolic byproducts and niche adjustment.
35 The complementary actions highlight the therapeutic potential of integrated probiotic-postbiotic
36 approaches for the enhancement of gut health.

38 **Keywords:**

39 Butyrate; *Lactiplantibacillus*; Postbiotic; Probiotic; Microbiome; Metabolism.



40 Introduction

41 Emerging gut microbiota-centric approaches, comprising probiotics (beneficial live
42 microorganisms), prebiotics (microbe-feeding), postbiotics (microbe-derived metabolites), and
43 synbiotics (synergistic combinations), are transforming translational research by facilitating a
44 favourable modulation of the host-microbiome axis to prevent or address metabolic, immune, and
45 neuropsychiatric disorders. By defining mechanistic pathways, such as the improvement of gut
46 barrier integrity, modulation of systemic inflammation, and production of bioactive compounds, these
47 interventions expedite the translation of microbiome research into targeted therapeutics and
48 personalized nutrition strategies ¹.

49 *Lactiplantibacillus plantarum* is one of the most extensively studied probiotics, which can
50 mitigate irritable bowel syndrome, diminish pathogenic bacterial burdens, and enhance the
51 prevalence of gut commensals (e.g., *Bifidobacterium*) and butyrogenic bacteria in clinical settings ².
52 Comparable to other probiotic bacteria, lactate produced by *L. plantarum* can be employed by cross-
53 feeding microorganisms to make butyrate ³, so indirectly affecting the gut metabolome.
54 Nevertheless, the probiotic efficacy may be limited by the survival of viable cells during
55 gastrointestinal transit, with viability reductions undermining therapeutic results. Short-chain fatty
56 acids (SCFA), especially butyrate, are a multifunctional postbiotic, produced during bacterial
57 fermentation of dietary fibers. Butyrate functions as the primary energy source for colonocytes,
58 improves mucosal barrier integrity by stabilizing hypoxia-inducible factor, and attenuates epithelial
59 permeability ⁴. Its immunomodulatory activities encompass the inhibition of histone deacetylases,
60 modification of regulatory T-cell differentiation, and reduction of pro-inflammatory cytokines ⁵. Pre-
61 clinical and clinical studies have shown that butyrate supplementation reduces the severity of colitis,
62 facilitates remission of inflammatory bowel disease (IBD), and safeguards against pathogen-induced
63 mucosal injury ⁶.

64 Probiotics utilize living microorganisms to provide health benefits through direct interactions
65 with the host and the generation of metabolites, whereas postbiotics, such as butyrate, eliminate the
66 necessity for microbial viability, providing benefits in terms of stability, safety, and uniformity.
67 Comparative research indicates that postbiotics may have more significant microbiome modulatory



68 effects in specific situations ⁷; nonetheless, comprehensive direct comparisons with probiotics under
69 controlled settings are scarce. Despite comprehensive research on both *L. plantarum* and butyrate,
70 it remains unclear whether the health-promoting effects of probiotic consumption are predominantly
71 attributable to live bacterial activity or metabolites like butyrate. Therefore, we hypothesized that
72 supplementation with *L. plantarum* and butyrate would induce unique but potentially complementary
73 alterations in gut microbiome composition and metabolite profiles using a novel *in vitro* pseudo-colon
74 system. Specifically, we hypothesize that *L. plantarum* will induce extensive alterations in microbial
75 diversity and competitively exclude opportunistic pathogens via live cell interactions and diverse
76 metabolite synthesis. Butyrate supplement, on the other hand, was expected to augment anti-
77 inflammatory metabolomic signatures without substantially modifying living community composition.
78 This direct comparison is expected to elucidate both overlapping and unique impacts, thereby
79 defining the degree to which butyrate facilitates the probiotic activities of *L. plantarum*. Collectively,
80 this direct comparison elucidates the gut-level mechanisms of probiotic-postbiotic action and guide
81 focused therapy options for gut health management.

82 **Materials and methods**

83 **Chemicals and reagents**

84 Gifu anaerobic medium and sodium butyrate were purchased from HiMedia, India. Oxgall,
85 sodium hydrogen carbonate, pancreatin, sodium sulphate, and n-hexane were acquired from LOBA
86 Chemie, India. N, O-Bis(trimethylsilyl)trifluoroacetamide was purchased from Sigma-Aldrich, USA.
87 Sodium hydroxide and hydrochloric acid for pH adjustment were purchased from Rankem, India.
88 Distilled water was obtained using the Millipore Milli-Q ultra-pure water (Ω 18.2) system.

89 **Functioning of the Artificial Colon Model for Microbiota Research (AMMR)**

90 To replicate the human colonic luminal microenvironment, we have designed and
91 developed a proprietary, fully customizable anaerobic gut microbiome culturing system named the
92 AMMR system (Indian design patent #394577-001; Indian patent application #202311013073; PTC
93 #PTC/IN2023/050834). The benefits of the anaerobic *in vitro* gut microbiome culturing system have
94 been recognized ⁸⁻¹¹ and applied for the understanding of microbiota and nutrient reciprocal



95 interactions independent of the host influence¹²⁻¹⁴. The AMMR system comprises two stainless-steel
96 modular units, left and right, each with dimensions of 540 mm (L), 215 mm (H). Each unit comprises
97 three independent interconnected anaerobic reactors mimicking the ascending, transverse, and
98 descending colon of the human intestine. The internal architecture of each reactor includes a
99 stainless-steel baffle with a bottom opening space for homogenous mixing of the fecal slurry and
100 mimicking the peristaltic movement of the human gut. The individual reactor vessel has a total
101 volume of 500 mL (400 mL of effective volume and 100 mL of headspace) and contains 5 ports
102 (1/4") each for pH sensor, headspace gas collection, liquid sample collection, gas purge, and feed
103 addition. The reactor lid with several access ports is connected to the vessel using autoclavable
104 gaskets and clamp-based seals, ensuring airtight closure. When not in use, each port is sealed to
105 maintain sterility and anaerobic conditions.

106 Both left and right units can be controlled by the common central control unit that
107 continuously monitors and regulates the reactor temperature and pH. Temperature control could be
108 achieved in the range of room temperature (~25 °C) to a maximum of 80 °C using an external water
109 jacket coupled with an integrated thermostat. The system can be used for both batch and fed-batch
110 modes of operation. Each of the six reactors is independently detachable from the adjacent reactors
111 for easy cleaning, sterilization and handling purposes. This configuration allows either for individual
112 operation of isolated reactors (representing a specific region of the intestine), or combined operation
113 of 3 reactors (representing ascending, transverse, and descending colon). A fed-batch and individual
114 operation approach was used for the current study. Adjacent reactors remain connected through
115 sealed connectors, allowing one-way flow of effluent. All the reactor chambers can be independently
116 flushed with N₂ gas to ensure an anaerobic environment for optimal *in vitro* gut microbial growth.

117 **Sample collection**

118 The following experiments were conducted under established rules and regulations. The
119 approval for the experiment was acquired from the Institutional Ethical Committee (TIET/EC/2023-
120 08). Informed consents were obtained from human participants of this study. All 5 donors
121 (**Supplementary Table 1**) were explained the experiment objectives and signed an informed
122 consent form for fecal matter donation, and a questionnaire regarding age, ethnicity, food type,



123 medical history, etc., was also obtained at the time of sample collection. The donors had not received
124 any antibiotic treatments or probiotic supplements for at least 3 months before donating the fecal
125 sample ¹⁵.

126 ***L. plantarum* strain acquisition and evaluation of probiotic characteristics**

127 *L. plantarum* MTCC 2621 (equivalent to ATCC 8014; *Lactiplantibacillus plantarum*) was
128 acquired from the Microbial Type Culture Collection (MTCC), Council of Scientific & Industrial
129 Research – Institute of Microbial Technology (CSIR-IMTech), Chandigarh, India, and was
130 cultured and maintained under standard conditions. These strains were stored as 20% glycerol
131 stock (v/v) in freezing conditions (–80 °C). The glycerol stock was used as the inoculum and
132 was grown in Gifu anaerobic medium, which was then used directly as the inoculum for
133 treatment.

134 **Experimental design**

135 Pooled fecal samples from n=5 individuals were used for the preparation of the stock fecal
136 slurry solution ¹⁶⁻¹⁹. In brief, morning fecal sample was collected individually from the donors in sterile
137 containers, pooled and mixed with Gifu anaerobic medium containing 13.5 g/L digested serum, liver
138 extract (1.2 g/L), 5 g/L soluble starch, L-cysteine hydrochloride (300 mg/L), sodium thioglycolate
139 (300 mg/L), soya peptone (3 g/L), and HM peptone B (2.2 g/L) ²⁰⁻²². Samples were homogenized in
140 the media and directly used for inoculation in the AMMR system through the entry port (**Fig. 1**).
141 Three independent reaction mixtures were prepared to evaluate the comparative probiotic and
142 postbiotic treatments on gut microbiota in terms of gut microbial population diversity and overall
143 metabolome: control group, butyrate (postbiotic) treated group, and *L. plantarum* (probiotic) treated
144 group (n=3 sets for each treatment). The chemical composition of each treatment was uniform, i.e.,
145 Gifu anaerobic medium (5.9%), oxgall powder (0.6%), sodium hydrogen carbonate (1.25%), and
146 pancreatin (0.1%) ²³. The pH of each of the reactors was maintained at 7.5 – 8.0, which critically
147 maintained the gut microbial populations ^{24, 25}. In *L. plantarum* treatment, 1X10⁶ CFU/mL was
148 inoculated, and 20 mM butyrate (corresponding to colonic concentration in healthy individuals) was
149 added for butyrate treatment ^{26, 27}. After feeding was done at 0-h, the reactors were flushed with N₂
150 gas and allowed to run for 48-h at 37 °C ^{28, 29}. Feeding of media was done every 4-h to maintain



151 optimal nutrient availability. After completion of the incubation period, samples were collected from
152 chamber 3 under aseptic conditions for metabolomic and metagenomic analysis.

153 **Sample preparation for untargeted metabolomics**

154 Gas Chromatography-Mass Spectrometry (GC-MS)-based untargeted metabolomics was
155 performed to elucidate the metabolic profile under each treatment. The culture media (2 mL) was
156 mixed with 2 mL of n-hexane and 100 μ L of N, O-Bis(trimethylsilyl)trifluoroacetamide, vortexed
157 vigorously for 30 min, and incubated at 40°C for 4-h at 200 rpm. The mixture was allowed to settle
158 down, the upper organic layer was separated, and centrifuged at 10,000 rpm for 15 min. The
159 supernatant obtained was mixed with a few granules of sodium sulfate, vortexed for 10 min, and
160 centrifuged at 10,000 rpm for 15 min. The resultant was filtered through 0.2 μ syringe filter, and
161 finally transferred to autosampler vials, sealed with a polytetrafluoroethylene cap.

162 **GC-MS analysis**

163 The metabolite extract was analyzed using SHS-40 instrument (Massachusetts, USA)
164 equipped with Bruker 436-GC series, SCION-SQ-MS model, and Rxi®-17Sil-ms column (30 m X
165 0.25 mm X 0.25 μ m). The initial temperature of the program was set at 60°C (solvent delay of 5 min)
166 with a hold of 4 min, followed by a ramp of 5°C/min, and the end temperature was set at 280°C with
167 a hold of 10 min. The derivatized samples (1 μ L) were injected in splitless mode, with a constant drift
168 of helium gas (1 mL/min). The MS transfer line temperature was kept at 280°C. Automated Mass
169 Spectral Deconvolution and Identification System (AMDIS) version 2.70 was used to analyze MS
170 data. Identification of major compounds was done based on mass fragmentation patterns (m/z) using
171 reference compounds in MS Interpreter version 2.0. The compounds were also matched with the
172 National Institute Standard and Technology (NIST) with an MS Library V2011. Metabolites identified
173 were filtered out based on a probability score of <60%.

174 **Metabolic pathway impact prediction**

175 Metabolic abundance data from GC-MS analysis were used for identifying metabolic
176 pathway impact using the Metaboanalyst V6 tool³⁰. Kyoto Encyclopedia of Genes and Genomes
177 (KEGG) was used as a reference library for pathway analysis and to evaluate how identified



178 metabolites significantly impact the general function of metabolic pathways based on the position
179 and connectivity of metabolites within the identified and impacted pathways. Identified compounds
180 were mapped against PubChem and KEGG identifiers.

181 **Metagenomic sequencing**

182 The reaction mixtures were processed for DNA isolation and 16S rRNA amplicon
183 sequencing. In brief, the DNA isolation was done using NucleoSpin Soil, Mini Kit (Cat# 740780,
184 MACHEREY-NAGEL GmbH & Co. KG) as per the manufacturer's instructions. DNA integrity
185 was evaluated using agarose gel electrophoresis and estimation of DNA concentration was done
186 using Qubit Quant-It dsDNA HS Kit on Qubit Fluorometer (Thermo Fisher). The V3-V4 region of the
187 16S rRNA genes was amplified by polymerase chain reaction with a universal forward primer and
188 unique barcode primer (bakt-341F: CCCTACACGACGCTCTTCCGATCTG-barcode-
189 CCTACGGGNGGCWGCAG; bakt-805R: GACTGGAGTTCCTTGGCACCCGAGAATTCCA-
190 barcode-GACTACHVGGGTATCTAATCC). The first amplification was performed using thermal
191 cycling conditions as below: 94 °C for 5 min; 5 cycles of denaturation at 94 °C for 30 s, annealing at
192 45 °C for 20 s, and elongation at 65 °C for 30 s; 20 cycles of denaturation at 94 °C for 20 s, annealing
193 at 55 °C for 20 s, and elongation at 72 °C for 30 s; and a final extension at 72 °C for 10 min. Illumina
194 bridge PCR compatible primers were introduced in the second amplification as follows: 3 min of
195 denaturation at 95 °C; 5 cycles of denaturation at 94 °C for 20 s, annealing at 55 °C for 20 s, and
196 elongation at 72 °C for 30 s; and a final extension at 72 °C for 10 min. Amplicons were purified using
197 AMPure XP beads, and Amplicon concentration was estimated using a Qubit 3.0 DNA Kit, 10 ng of
198 amplicons from each sample were sequenced using the Illumina MiSeq 2 × 300 bp platform.

199 **16s rRNA sequence data analysis**

200 Sequence data were analyzed using Quantitative Insights into Microbial Ecology (QIIME
201 v2) by excluding primers and spacers from the sequences as previously outlined^{31, 32}. The Divisive
202 Amplicon Denoising Algorithm 2 (DADA2) was used for trimming, denoising, merging the forward
203 and reverse reads (paired-end), and removing chimeric sequences. OTU clustering was performed
204 on denoised sequences using the q2-vsearch function in the QIIME2 pipeline. Forward and
205 reverse reads were discarded if their quality was poor (Q<25%). The obtained feature table was



206 rarefied using the diversity core-metrics-phylogenetic (q2-diversity) plugin in QIIME2 at a sample
207 depth of 12,000 to calculate microbial diversity. The diversity of microorganisms across different taxa
208 was elucidated by using the readings from the feature table and reference taxonomic annotations
209 from the SILVA database (version 138). Reads were obtained with 99% 16S coverage and raw
210 taxonomy files that were trained using the Naive Bayes classifier. The trained classifier was later
211 used using representative sequences produced by DADA2 to allocate sequences to certain taxa.
212 Sequences constituting 0.5% of low abundance were omitted from all cases. The enrichment of
213 microbial metabolic pathways was calculated using 16S rRNA sequences using the Phylogenetic
214 Investigation of Communities by Reconstruction of Unobserved States (PICRUSt). Operational
215 Taxonomic Units (OTUs) were aligned with the GreenGenes database (gg_13_08) using QIIME2,
216 using a 97% similarity criterion and closed OTU selecting methodology. The abundance of OTUs
217 was calibrated to the 16S rRNA gene copy number obtained from recognized bacterial genomes in
218 Integrated Microbial Genomes. Anticipated functions were aligned using the Kyoto Encyclopedia of
219 Genes and Genomes (KEGG) database.

220 **Statistical analysis**

221 GraphPad V8 was used for statistical analysis of data, and quantitative data were
222 interpreted as mean \pm SEM. Metaboanalyst V6 was used for biochemical pathway enrichment
223 utilizing a metabolite abundance list obtained from GC-MS analysis³³. The enrichment ratio (ER) for
224 the subclass was computed using observed hit/expected hit values. Holm-Bonferroni correction for
225 P-value and false discovery rate (FDR) was computed for each enrichment analysis entry. $P < 0.05$
226 was considered significant. A linear correlation between any two independent variables was done
227 using Pearson's method. The KEGG database was used as a reference library for pathway analysis
228 to examine functionally related metabolites and their considerable enrichment. This analysis focused
229 on the identification of metabolites that could prevent the requirement for preselecting metabolites
230 based on arbitrary cut-off thresholds³⁴. The identified metabolites were cross-referred with
231 PubChem and KEGG identifiers. Pathway analysis was done using Fisher's exact test, and pathway
232 impact was calculated based on the topological importance of different metabolites in a certain
233 pathway. The metabolome and microbiome data were log-transformed and mean-centered



234 normalized for one-factor analysis to get equal variance. The differences in microbial communities
235 and metabolites in different treatments were analyzed using STAMP v2.1.3. For comparison, t-test
236 (equal variance) with a p-value filter (>0.05) was used. Extended error bar plots were made to show
237 statistically significant values, Welch's confidence intervals, and differences in mean proportion
238 effect size.

239 Results

240 Microbiome profile

241 Both butyrate and *L. plantarum* differentially altered the gut microbial architecture at various
242 taxonomic levels compared to control. At the phylum level, five considerable phyla were identified,
243 and the gut microbiota in all three groups were predominantly composed of Firmicutes (43.61%),
244 Bacteroidetes (35.28%), and Proteobacteria (14.31%) (**Fig. 2A**). Although low in abundance,
245 Tenericutes were observed to be uniquely identified in *L. plantarum*, indicating enrichment of specific
246 species associated with the Tenericutes phylum. Compared to the control, we found that butyrate
247 induced a 12.0% reduction in Firmicutes and a 4.3% decrease in Bacteroidetes, accompanied by a
248 49.6% increase in Proteobacteria. Conversely, *L. plantarum* resulted in a 7.4% decrease in
249 Firmicutes, an 8.9% increase in Bacteroidetes, and a minor 3.9% rise in Proteobacteria, with
250 negligible impacts on other phyla. As a result, the Firmicutes:Bacteroidetes (F:B) ratio demonstrated
251 a trend of reduction due to the treatments *i.e.*, initially 1.34 in control, decreased to 1.23 ($P=0.35$)
252 following butyrate treatment and to 1.14 ($P=0.12$) due to *L. plantarum*.

253 At the order level (**Fig. 2B**), a total of 37 orders were detected. In the control group, the gut
254 microbiota was predominantly composed of Lactobacillales (41.55%), Bacteroidales (34.74%), and
255 Enterobacterales (12.12%). Following butyrate treatment, the microbial community was different,
256 resulting in Bacteroidales (33.18%), Enterobacterales (18.07%), and Clostridiales (15.60%)
257 emerging as the predominant groups, due to butyrate's established ability to influence gut microbial
258 composition through anti-inflammatory short-chain fatty acid signaling. The treatment with *L.*
259 *plantarum*, in contrast, reinstated a profile similar to the controls - Bacteroidales (37.82%),
260 Lactobacillales (37.63%), and Enterobacterales (12.60%) - demonstrating its capacity for probiotic-



261 induced community rearrangement. A direct comparison of the two interventions on the principal
 262 orders revealed that butyrate causes suppression of Lactobacillales (4.23% vs. 37.63%),
 263 moderately reduced Bacteroidales (33.18% vs. 37.82%), and increased Enterobacterales (18.07%
 264 vs. 12.60%) in relation to *L. plantarum*, underscoring the contrasting effects of a postbiotic compared
 265 to a live probiotic on essential gut taxa.

266 In case of genus, 145 genera were identified, of which 75, 108, and 64 absolute genera
 267 were identified in control, butyrate, and *L. plantarum* treatments, respectively, indicating an
 268 increased microbial diversity in butyrate treatment. In the control group, the three most abundant
 269 genera were found to be *Enterococcus* (39.2%), *Bacteroides* (33.7%), and *Klebsiella* (6.9%); in the
 270 butyrate treatment, the top three genera were *Bacteroides* (30.1%), *Peptoniphilus* (6.94%) and
 271 *Lachnoclostridium* (4.25%), whereas in the *L. plantarum* group the dominant genera were
 272 *Enterococcus* (37.3%), *Bacteroides* (36.9%), and *Klebsiella* (7.9%) (**Fig. 2C**). *Pectobacterium*
 273 (0.022%), *Flavonifractor* (2.207%), and *Micrococcus* (0.003%) were the most unique genera as
 274 identified in control, butyrate, and *L. plantarum* groups, respectively, having the highest abundance
 275 among all the unique genera. While increasing *Parabacteroides* (0.008 – 1.55%) and certain
 276 butyrate-producers like *Blautia* (0.017 – 0.137%) and *Butyricicoccus* (0 – 0.005%), we observed a
 277 slight drop in *Bacteroides* after butyrate supplementation as compared to control as well as notable
 278 decreases in classic pathobionts *Enterococcus* (39.2 → 4.0%), *Klebsiella* (6.9 → 0.01%), and
 279 *Enterobacter* (0.60 → 0.009%) were also inferred. By comparison, *L. plantarum* treatment showed
 280 increased *Bacteroides* and *Klebsiella* but mostly maintained high *Enterococcus* levels and had no
 281 impact on *Escherichia* and *Enterobacter*. We deduced that butyrate therapy thereby changed the
 282 gut microbiota toward lower possible pathogens and increased SCFA producers; *L. plantarum*
 283 strengthened important butyrate-producing taxa but had little effect on pathobiont suppression.

284 Fifteen and four differential genera were identified between control and butyrate treatment
 285 and control and *L. plantarum* treatment, respectively (**Fig. 2D-F**). Of note, the mean proportion of
 286 *Lachnoclostridium* ($p < 0.05$) was seen to be significantly higher in butyrate treatment (**Fig. 2D**) and
 287 significantly lower in *L. plantarum* treatment (**Fig. 2E**) when compared to the control. Butyrate
 288 treatment showed significant enrichment of *Bacteroides* (**Fig. 2D, F**), and *L. plantarum* treatment



289 showed significant enrichment of *Klebsiella* (**Fig. 2E, F**). The correlation heatmap of the top 50
290 genera with the highest abundance across the treatments showed a close association between
291 control and *L. plantarum* treatment at the gut microbiome level. Our data indicates that butyrate
292 treatment is positively correlated with butyrogenic and fiber-degrading genera, i.e., *Intestinimonas*,
293 *Clostridium*, *Ruminococcus*, *Shigella*, etc., while some of them are negatively correlated, like
294 *Roseburia*, *Eubacterium*, *Faecalibacterium*, etc. (**Fig. 2G**). In contrast, lactic acid-associated genera
295 like *Lactonifactor*, *Bacteroides*, *Lactobacillus*, etc., were observed to be positively correlated with *L.*
296 *plantarum* treatment, and negatively correlated with butyrate treatment, indicating specific
297 enrichment of lactic acid bacteria in *L. plantarum* treatment.

298 **Microbial metabolic functions**

299 Significant differences in various microbial metabolic functions were computed under
300 butyrate and *L. plantarum* treatment, compared to the control (**Fig. 3**). In our results, butyrate
301 treatment was found to redirected microbial metabolism from antibiotic and fatty acid biosynthesis
302 to amino acid synthesis, energy metabolism, and motility (**Fig. 3A**). For instance, butyrate showed
303 significantly increased processes associated with amino acid synthesis and central energy
304 metabolism. The biosynthesis of valine, leucine, and isoleucine has shown a significant rise in
305 addition to histidine metabolism, alanine, aspartate and glutamate metabolism, and pantothenate
306 and CoA biosynthesis. Energy pathways such as carbon fixation via the citrate cycle (TCA cycle)
307 show minor enrichments. Critical pathways for antibiotic synthesis were seen to be significantly
308 downregulated. The production of vancomycin group antibiotics decreased considerably, as did the
309 biosynthesis of streptomycin. The production of secondary bile acids was depleted under butyrate
310 treatment. *L. plantarum* treatment showed limited alterations in gut microbial metabolic functions
311 which included enrichment of pathways pertaining to ascorbate and aldarate metabolism, and
312 nucleotide excision repair, while a depletion in glycosaminoglycan degradation, histidine
313 metabolism, and taurine and hypotaurine metabolism was noted in *L. plantarum* group compared to
314 control (**Fig. 3B**). Distinct difference in microbial function was also observed between butyrate and
315 *L. plantarum* groups (**Supplementary fig. 1**). A total of 113 common microbial metabolic functions
316 were predicted, out of which 1 and 7 were unique in control and butyrate treatment, respectively (**Fig**



317 **3C)**. Association heatmap coupled with sample clustering clearly indicated a close association
318 between control and *L. plantarum* group, whereas butyrate resulted in altered microbial function,
319 which was different from that of control and *L. plantarum* (**Fig. 3D**).

320 **Untargeted metabolomic profile**

321 A total of 44, 39, and 51 metabolites were identified in control, butyrate, and *L. plantarum*
322 groups, respectively (**Fig. 4A**) (**Supplementary Tables 5-7**). Although they differed in abundance,
323 octanoic acid and capric acid were the top-abundant metabolites in all groups, followed by indole in
324 control and butyrate, and gln-glu peptide in *L. plantarum*. Seven metabolites were common among
325 the treatments with variable abundance (**Fig. 4B**) (**Supplementary Table 8**). These metabolites
326 include indole, homovanillic acid, octanoic acid, capric acid, phenylacetylglycine, D-galactose, and
327 nonanoic acid. Although the abundance of these metabolites differed across treatments, a significant
328 difference in mean proportion was observed only in the case of indole, capric acid, nonanoic acid,
329 and octanoic acid (**Fig. 4C-E**). The mean proportion of capric acid and octanoic acid ($p < 0.05$) was
330 observed to be significantly less in the butyrate treatment (**Fig. 4C**), but higher in the *L. plantarum*
331 treatment (**Fig. 4D**) in comparison to the control group. The mean proportion of indole was
332 significantly higher in the butyrate treatment than control and *L. plantarum* treatment (**Fig. 4C, E**).
333 Unlike the correlation heatmap of genera identified and microbial metabolic functions for various
334 treatments, the correlation heatmap of the top 50 highly abundant metabolites showed that control
335 and butyrate treatment confer a close association in terms of metabolome data (**Fig. 4F**). It was seen
336 that some of the metabolites showed similar patterns of correlation in both butyrate and *L. plantarum*
337 treatments. Homovanillic acid, nonanoic acid, methyl acetate, methyl propionate, p-cresol, palmitic
338 acid, etc., showed positive correlation, and phenylacetylglycine, and several peptides like asn-asn-
339 lys, trp-glu, etc., showed negative correlation with both the treatments in comparison to the control.
340 Specifically, in *L. plantarum* treatment, 9-octadecenoic acid, acetic acid, indole-3-carboxylic acid,
341 etc., showed positive correlation, and urea, stearic acid, L-saccharopine, indole, etc., showed
342 negative correlation. Similarly, in butyrate treatment, N-acetylputrescine, caproic acid,
343 propionamide, etc., showed positive correlation, and capric acid, octanoic acid, D-galactose, myristic
344 acid, etc., showed negative correlation. The control group exhibited baseline correlations with



345 fermentation byproducts (2,3-hexanediol) and higher aromatic metabolites, indicating unmodulated
346 gut metabolism.

347 **Chemical class enrichments**

348 Based on the identified metabolites, respective chemical class enrichments were identified.
349 It was found that amino acid, peptides, and analogues was significantly enriched in control, and fatty
350 acids and conjugates in butyrate and *L. plantarum* treatments (**Fig. 4H-J**) (**Supplementary Tables**
351 **9-11**), followed by fatty acids and conjugates in control, carbonyl compounds in butyrate and amino
352 acids, peptides and analogues in *L. plantarum* treatment as second significant metabolite class. In
353 terms of enrichment ratio, the control group showed higher enrichment of alloxazines and
354 isoalloxazines, purine nucleosides, and dibenzylbutanediol lignans (**Fig. 4H**). Similarly, for the
355 butyrate group, phenylacetic acid, carboximidic acids, and cresols have a high enrichment ratio (**Fig.**
356 **4I**); and pyrimidine ribonucleosides, cinnamic acids, and pyridines were highly enriched for the *L.*
357 *plantarum* group (**Fig. 4J**). A total of 6 metabolite classes were common across the three groups,
358 while 6, 5, 12 metabolite classes were inferred to be distinctly enriched in control, butyrate, and *L.*
359 *plantarum* treatment, respectively (**Fig. 4G**) (**Supplementary Table 12**).

360 **Metabolic pathway enrichments**

361 The identified metabolites were mapped against the KEGG as a reference library for further
362 identification of impacted pathways. The examination of metabolic pathway enrichment
363 demonstrates unique patterns across the control, butyrate, and *L. plantarum* groups. The pathway
364 impact analysis showed that in control, the top 3 highly impacted pathways include riboflavin
365 metabolism (impact=0.11), D-amino acid metabolism (impact=0.05), and pyrimidine metabolism
366 (Impact=0.04) (**Fig. 5A**) (**Supplementary Table 13**). In butyrate group, the top 3 highly impacted
367 pathways comprise phenylalanine, tyrosine and tryptophan biosynthesis (impact=0.04), propanoate
368 metabolism (Impact=0.04), and pentose phosphate pathway (impact=0.02) (**Fig. 5B**)
369 (**Supplementary Table 14**). The same in *L. plantarum* group includes D-amino acid metabolism
370 (impact=0.17), valine, leucine and isoleucine degradation (impact=0.15), and taurine and
371 hypotaurine metabolism (Impact=0.14) (**Fig. 5C**) (**Supplementary Table 15**). Six metabolic



372 pathways were found to be common among all treatments. In contrast, butyrate showed specific
373 enrichment of pentose phosphate pathway (Fig. 5D) (Supplementary Table 16).

374 Discussion

375 The current study was conducted to infer the differential effects of *L. plantarum* (butyrogenic
376 probiotic)³⁵ and butyrate (postbiotic) on gut microbial population and diversity, metabolites, and
377 associated metabolic pathways using metagenomics and metabolomics approaches. Our results
378 indicate that *L. plantarum* and butyrate exhibit distinct yet complementary effects on gut microbes,
379 suggesting that both live bacteria and metabolic byproducts of *L. plantarum* can confer health
380 benefits.

381 The human colon, possessing the greatest microbial density among human-associated
382 microbial communities, offers a stable anaerobic environment for many bacterial populations vital to
383 host physiology³⁶. Comprehending colonic biogeography and host-microbe interactions is
384 fundamental to translational microbiome research and clinical treatment advancements, hence
385 improving metabolic resilience. Nevertheless, research on pre-clinical and clinical colonic
386 microbiomes studies exhibits significant variation, which is attributed to individual host characteristics
387 (e.g., genetics, immunological status), variations in housing and feeding, and uncontrolled
388 fluctuations in luminal composition^{37, 38}. Variations in transit durations, pH gradients, and mucus
389 layers further induce compositional alterations, complicating comparison analysis among cohorts.
390 Microbial interactions with leftover feed, bile salts, and host-secreted substances create uncontrolled
391 chemical heterogeneity within the lumen³⁹. These confounding variables compromise the
392 reproducibility and translational validity of pre-clinical findings. Consequently, rigorously regulated,
393 standardized *in vitro* or gnotobiotic models with entirely chemically specified luminal inputs are
394 crucial to eradicate variability and facilitate reliable, reproducible mechanistic understanding. For
395 strict gut microbial control to eliminate unnecessary variability, various *in vitro* strategies have been
396 developed over the years to emulate the intricacies of the human gastrointestinal tract, addressing
397 the shortcomings of fecal batch cultures and animal models^{9, 40, 41}. These multicompart dynamic
398 systems facilitate standardized luminal conditions and continuous or batch feeding, hence



399 minimizing variability arising from host variables, luminal heterogeneity, and environmental
400 variations. Thus, these *in vitro* models provide a consistent mechanistic understanding of microbial
401 metabolism, host-microbe interactions, and the effectiveness of interventions in gut microbial
402 research.

403 According to 16S rRNA gene sequencing data, *L. plantarum* reshaped the gut microbial
404 community, irrespective of a considerable impact on the overall microbial diversity. This observation
405 aligns with the previous pre-clinical and clinical reports that probiotics, especially belonging to the
406 genus *Lactobacillus* may exert health-beneficial effects without impacting the gut microbial diversity
407 ^{42, 43}. In fact, an earlier study indicated that supplementation of a single probiotic sp. may not be
408 efficient enough to improve the overall diversity of the gut microbiota ⁴⁴. This strict nature of the gut
409 microbiota, especially within the closed AMMR system, could result due to causes such as niche
410 occupation without displacing other community members, transient colonization and impact on the
411 entire microbiota population, resilience nature of the core microbiome preventing displacement and
412 colonization success by *L. plantarum*, and innate compensatory dynamics of the gut microbiota
413 where functionally analogous spp. may bloom upon *L. plantarum*-mediated suppression of specific
414 genera ^{45, 46}.

415 On the contrary, butyrate treatment tends to increase the gut microbial diversity (108 vs.
416 75) due to improved energy metabolism and cross-feeding in the gut microbial population ⁴⁷. Butyrate
417 is a metabolic end-product of primary fermenters (e.g., *Faecalibacterium*, *Roseburia*), which is then
418 used as an energy source by secondary microbial consumers ⁴⁸. This establishes interconnected
419 trophic networks in which butyrate supports auxotrophic organisms that lack the ability for primary
420 fibre breakdown. This cross-feeding enhances niche specialization and stabilizes community
421 structure, hence directly augmenting microbial diversity ⁴⁹. It ecologically converts butyrate into a
422 communal resource that supports mutualistic relationships.

423 Differential alteration at the microbial taxonomic levels was noted by butyrate and *L.*
424 *plantarum*. The increased abundance of Proteobacteria observed following butyrate treatment
425 remains aligned with previous reports ²⁷. Although the bloom of Proteobacteria has historically been
426 associated with mucosal inflammation and gut-barrier dysfunction due to the presence of pyrogenic



427 endotoxin, recent studies indicate diverse beneficial role of Proteobacteria that includes the
428 production of essential vitamins ⁵⁰, providing colonization resistance ⁵¹, and metabolic signaling ⁵².
429 Tenericutes was identified only under *L. plantarum* treatment, and this aligns with previous report
430 that lactic acid bacteria favor the growth of Tenericutes ⁵³. Our data show a decreased trend of F:B
431 ratio ($P>0.05$) after probiotic and postbiotic treatments. This is important since increased F:B ratio is
432 often associated with obesity ^{54, 55}, and previous studies also showed that probiotic treatment
433 generally decreases F:B ⁵⁶.

434 At the order level, the populations of Clostridiales, Veillonellales, and Enterobacterales
435 were distinctly enriched due to butyrate treatment. Various members of the Clostridiales order,
436 especially butyrate-producing species, may directly use butyrate as an energy substrate or a
437 signaling molecule to enhance their growth and activity ⁵⁷. Within the AMMR system, where the
438 nutrient availability is tightly controlled and other metabolic substrates are restricted, the direct supply
439 of butyrate might provide a competitive advantage to these organisms, resulting in population
440 growth. Butyrate increased the population of Veillonellales, which generally does not synthesize or
441 utilize butyrate, but uses lactate, which is a prevalent byproduct of carbohydrate fermentation by
442 anaerobes in the gut ⁵⁸. If butyrate addition increased the proliferation of primary fermenters that
443 generate lactate, then Veillonellales would subsequently grow owing to increased substrate
444 availability. Butyrate may also affect the community's general metabolic activity, resulting in
445 alterations in fermentation pathways that promote lactate generation. Indeed, our data show an
446 increased population of Bacteroides under butyrate treatment, which is an obligate anaerobe and
447 follows a fermentative mode of energy production ⁵⁹. Interestingly, butyrate resulted in suppression
448 of Lactobacillales, a surprising and quite uncommon observation. Lactobacillales are well-studied
449 lactate-producing bacteria and butyrate is typically produced due to lactate fermentation by gut
450 microbes ⁶⁰. Consequently, the reduction in lactate-producing microbial orders may result from
451 feedback inhibition caused by butyrate accumulation during feeding or from the acidic pH of the
452 medium created by butyrate (a weak acid), as many lactate-producing species exhibit sensitivity to
453 pH levels. At genus level, control and *L. plantarum* groups showed similar patterns for enriched
454 genera, but butyrate group showed high abundance of *Peptoniphilus* and *Lachnoclostridium* in



455 comparison to control and *L. plantarum*. Both are butyrate-producing bacteria and display anti-
456 inflammatory properties ^{61, 62}. Butyrate supplementation lowers the pH of the medium, favoring the
457 growth of butyrate-producing bacteria ⁶³ and also decreases the abundance of known pathobionts
458 (*Enterococcus*, *Klebsiella*, and *Enterobacter*). The mean proportion of *Bacteroides* and *Klebsiella*
459 was enriched in butyrate and *L. plantarum* treatment, respectively. *Bacteroides* is a known butyrate-
460 producing genus ^{64, 65}, and evidence for increased *Klebsiella* after probiotic treatment is not present
461 in the literature. The possible explanation for this observation could be that probiotic treatment
462 conferred decreased microbial diversity that normally suppresses *Klebsiella*, causing a possibility of
463 niche expansion for it.

464 Metabolomics data revealed the highest enrichment of octanoic acid and capric acid in all
465 treatments, referring to the healthy metabolome of the gut microbial population ^{66, 67}. The presence
466 of indole and p-cresol in high concentration in butyrate and *L. plantarum* treatments indicates
467 reduced carbohydrates and increased ammonium levels, potential markers for proteolytic
468 metabolism ⁶⁸. This could explain the possible reason for the identification of various peptides, like
469 thr-leu, gln-glu, etc., in both treatments. Capric and octanoic acids are the saturated fatty acids
470 whose mean proportion was found to be higher in *L. plantarum* treatment in comparison to butyrate.
471 Previous studies confirm that fatty acid metabolism and the saturation mechanisms of fatty acids
472 were prominent in *L. plantarum* ⁶⁹, while butyrate inhibits saturated fatty acids formation and
473 accumulation ⁷⁰. *L. plantarum* produces organic acids like lactic acid and acetic acid ⁷¹, and in our
474 results, we found a positive correlation between *L. plantarum* treatment and acetic acid. In a previous
475 study utilizing *L. plantarum* for the treatment of high-fat-induced obesity in mice, indole-3-carboxylic
476 acid was found to be one of the significant metabolites associated with *L. plantarum* treatment ⁷²,
477 which confirms a positive association between indole-3-carboxylic acid and *L. plantarum* treatment
478 as found in our study. In case of butyrate treatment, a positive correlation was found with N-
479 acetylputrescine, a polyamine, and caproic acid, a saturated fatty acid. The correlation between
480 butyrate and polyamines is well studied, and in an experiment utilizing mouse colon cancer cells, it
481 was found that butyrate treatment enhances the production of polyamines ⁷³. Additionally, a study



482 by Nzeteu *et al* explains how lactic acid and butyric acid biomass produced in a similar closed
483 anaerobic system can help in increased production of caproic acid ⁷⁴.

484 Chemical class enrichment for each treatment revealed the significant enrichment of fatty
485 acids and conjugates in both butyrate and *L. plantarum* treatments. In line, previous study also
486 claimed that probiotic bacteria can produce anti-inflammatory fatty acid conjugates to treat colitis ⁷⁵.
487 Butyrate favors the growth of SCFA-producing bacteria ⁶³, and with increased SCFA levels would
488 lead to enrichment of fatty acids. As previously mentioned, identification of indole and p-cresol in
489 butyrate and *L. plantarum* indicates proteolytic activities ⁶⁸. This justifies the identification of
490 phenylacetic acid, an intermediate of phenylalanine metabolism, as the highest enriched chemical
491 class and phenylalanine, tyrosine, and tryptophan biosynthesis as highly impacted pathways in
492 butyrate treatment ⁷⁶. Also, in *L. plantarum* treatment, the top three impacted pathways are related
493 to protein and amino acid metabolism. Butyrate shows specific enrichment of the pentose phosphate
494 pathway, which aligns with the previous results demonstrating the role of butyrate in higher
495 expression of glucose-6-phosphate dehydrogenase, a key enzyme in the pentose phosphate
496 pathway, for nucleic acid synthesis and reactive oxygen species generation to initiate host defense
497 ⁷⁷.

498 The gut microbial metabolic functions based on KEGG functional orthologs were computed
499 using sequence data and further validated using the metabolomic profile. Several commonly
500 enriched microbial pathways were identified using both approaches, while uniquely enriched
501 pathways were identified across treatments. For instance, galactose, lipoic acid, and pyruvate
502 metabolic pathways are universally enriched since they represent fundamental energy and redox
503 modules in gut microorganisms ^{78, 79}. Galactose catabolism generates glucose-6-phosphate for
504 glycolysis, facilitating ATP production via substrate-level phosphorylation and producing NADH that
505 propels subsequent oxidation ⁸⁰. The pyruvate metabolism is crucial since the pyruvate
506 dehydrogenase complex irreversibly decarboxylates pyruvate to acetyl-CoA, connecting glycolysis
507 to the TCA cycle for optimal ATP production by oxidative phosphorylation ⁸¹. These processes



508 produce NADH and FADH₂, whose reoxidation (via respiration or fermentation) maintains the
509 NAD⁺/NADH equilibrium. Under anaerobic conditions, gut bacteria often convert pyruvate to lactate
510 or ethanol to produce NAD⁺, hence directly associating these pathways with redox equilibrium ⁸².
511 Lipoic acid is an essential cofactor for pyruvate dehydrogenase and other 2-ketoacid
512 dehydrogenases, linking carbon metabolism to electron transport; its redox-active disulfide bond
513 also connects metabolism to oxidative stress responses ⁸³. These mechanisms together provide
514 energy carriers (ATP), reducing equivalents, and biosynthetic precursors, constituting preserved
515 "housekeeping" capabilities essential for microbial growth and survival. Consequently, all groups
516 exhibit enrichment in these pathways as shown by KEGG annotations. Nevertheless, the elevated
517 enrichment in control and *L. plantarum* groups, relative to butyrate, likely indicates active
518 carbohydrate fermentation within those communities. *L. plantarum* and other fermentative organisms
519 depend on efficient glycolytic and PDH/lipoate mechanisms to extract energy from carbohydrates.
520 In contrast, the butyrate-treated group exhibited reduced enrichment, likely attributable to metabolic
521 feedback and alterations in community dynamics. Exogenous butyrate may undergo β-oxidation to
522 provide acetyl-CoA, which directly energizes the TCA cycle, potentially meeting energy requirements
523 and inhibiting glycolysis/galactose metabolism via end-product feedback mechanisms ⁸⁴. Moreover,
524 butyrate may promote SCFA-utilizing taxa to the detriment of sugar-fermenters, hence modifying
525 substrate availability ⁸⁵. This feedback control and microbial turnover may reduce the incidence of
526 galactose utilization and PDH-dependent genes.

527 In the butyrate-treated group, butyrate likely played a central role as a regulatory signal and
528 favored energy substrate for gut microorganisms. Its presence within the closed system could be
529 sensed as excess energy availability, resulting in feedback inhibition. In line, glycolysis and
530 gluconeogenesis diminish since butyrate was the direct energy source (acetyl-CoA), hence
531 lessening the need for glucose catabolism or anabolism ⁸⁶. Fatty acid biosynthesis was inhibited
532 because butyrate, a fatty acid derivative, satisfied the requirement for additional fat ⁸⁷. The
533 metabolism of lipoic acid, essential as a cofactor in primary energy pathways such as pyruvate
534 dehydrogenase (connecting glycolysis to the TCA cycle), subsequently diminishes when these



535 fundamental energy-producing mechanisms become less requisite in the presence of enough
536 butyrate⁸⁸. This signifies a transition towards energy conservation and the exploitation of available
537 butyrate.

538 However, in the case of *L. plantarum* treated group, the augmentation of certain microbial
539 metabolic pathways may be ascribed to its diverse interactions with the gut microbiota. For instance,
540 *L. plantarum* enhances pyruvate metabolism and glyoxylate/dicarboxylate metabolism likely by
541 acting as a trigger for glycolysis, decomposing available carbohydrates into pyruvate and
542 phosphoenolpyruvate⁸⁹. These intermediates can enter the glyoxylate shunt, circumventing
543 decarboxylation stages in the TCA cycle, hence facilitating efficient carbon utility for biosynthesis
544 under low-energy circumstances. Simultaneously, other carbon fixation pathways are enhanced to
545 facilitate anaplerotic metabolic reactions, restoring oxaloacetate and succinate for the synthesis of
546 amino acids and nucleotides⁹⁰. The enhancement of valine, leucine, isoleucine, and
547 alanine/aspartate/glutamate metabolism under *L. plantarum* can provide essential substrates for
548 microbial growth and colonization⁹¹. Branched-chain amino acids (BCAAs) act as nitrogen donors
549 for several metabolic pathways⁹², while glutamate produces glutathione⁹³. Under *in vivo* conditions,
550 the metabolism of arginine and proline can facilitate collagen synthesis and immune cell
551 communication⁹⁴, consistent with *L. plantarum*'s established function in improving mucosal integrity
552⁹⁵. *L. plantarum*-induced enhancement of sulfur metabolism and taurine/hypotaurine metabolism
553 could help alleviate oxidative stress⁹⁶. The reduction of sulfur produces hydrogen sulfide, which, at
554 healthy concentrations, can activate antioxidant mechanisms. Taurine and hypotaurine metabolism,
555 enhanced under *L. plantarum*, can function as an effective ROS quencher. This is crucial in
556 inflammatory environments since *L. plantarum* inhibits pro-oxidant pathogens. Collectively, *L.*
557 *plantarum* functions as a metabolic coordinator, enhancing cross-feeding networks that maximize
558 energy extraction, redox equilibrium, and structure biosynthesis, thereby explaining the extensive
559 upregulation of several interrelated pathways.



560 Finally, it is to be noted that the current observations emerged out of an *in vitro* anaerobic
561 culture system. Although the AMMR system is able to strictly control certain biochemical parameters
562 of the human distal intestine, instruments like these, are unable to capture the totality of the intricate
563 and dynamic host-microbe interaction that is influenced by various physiological conditions like gut
564 epithelial response, mucus layer dynamics, hormonal levels, immune cell signalling and
565 metabolomic crosstalk. Additionally, the efficacy of probiotics and postbiotics is inherently connected
566 to their nutritional context and food matrix. Their metabolic fate is influenced by intricate interactions
567 within the specific functional food matrix, which includes various nutrients, fibers, and metabolites
568 present. Consequently, outcomes observed in a specific formulation or a simplified experimental
569 model may not reliably predict their behaviour in a different food or within the human gut.
570 Nevertheless, the current study provides preliminary glimpse of how probiotic and postbiotic
571 differentially impacts the gut microbiota in an host-independent controlled environment. Further, *in*
572 *vivo* intervention studies are essential to validate these results.

573 Conclusion

574 This study elucidates distinct roles of butyrate and *L. plantarum* on gut microbial activities
575 and community composition within an *in vitro* colonic model named AMMR system. Butyrate
576 markedly increased total microbial diversity, likely due to improved cross-feeding, whereby butyrate
577 acts as an energy substrate for secondary fermenters, promoting trophic networks and niche
578 specialization. It inhibited both Firmicutes and Bacteroidetes while enhancing the abundance of
579 Proteobacteria and Actinobacteria. In addition, a reduction in harmful genera (e.g., *Enterococcus*,
580 *Klebsiella*, *Enterobacter*) was observed while selectively fostering beneficial butyrogenic taxa (e.g.,
581 *Lachnospirillum*, *Blautia*). Butyrate functionally switched metabolism from antibiotic and fatty acid
582 biosynthesis to amino acid synthesis (valine, leucine, isoleucine, histidine), energy pathways
583 (propanoate metabolism, pentose phosphate pathway), and motility, while reducing secondary bile
584 acid production (suppression of inflammatory metabolic pathways). The metabolomic profile
585 exhibited a correlation with N-acetylputrescine and caproic acid, indicating modifications in
586 polyamine and fatty acid metabolism. Conversely, *L. plantarum* maintained community diversity



587 similar to the control, exerting small influence on the F:B ratio or prospective pathobionts (e.g.,
588 *Enterococcus*). It enhanced Bacteroidetes and lactic acid bacteria, and metabolically elevated redox
589 balance pathways (taurine/hypotaurine metabolism, sulfur metabolism) and amino acid breakdown
590 (valine, leucine, isoleucine), while diminishing glycosaminoglycan destruction. The metabolome
591 exhibited a favorable association with acetic acid and indole-3-carboxylic acid, consistent with its
592 lactic acid synthesis. In contrast to butyrate, *L. plantarum* augmented pyruvate and glyoxylate
593 metabolism, facilitating carbon fixation and biosynthesis under low-energy conditions. Collectively,
594 the findings of the study reveal that butyrate primarily functions as a metabolic regulator, influencing
595 community composition and functionality via metabolic feedback and cross-feeding, diminishing
596 pathogens and promoting energy and amino acid metabolism. *L. plantarum*, on the other hand,
597 functioned as a metabolic coordinator, enhancing lactic acid bacteria and stress-response pathways
598 without significantly modifying diversity or pathogen abundance. Therefore, the combined
599 application of both probiotic strain and postbiotic metabolite may provide a promising basis for
600 symbiotic formulations for enhanced gut homeostasis and alleviate gut associated metabolic
601 disorders.

602

603 **Acknowledgement:** Financial assistance from Biotechnology Industry Research Assistance
604 Council (BIRAC/FITT01085/BIG-20/22) is acknowledged.

605

606 **Conflict of interest:** The AMMR system is the proprietary item of Fermibio Solutions Private
607 Limited, with which Priyankar Dey & Prangya Ranjan Rout are affiliated.

608

609 **Contribution:** NB performed the experiments, conducted the analysis and wrote the 1st draft of the
610 manuscript along with PD; PRR edited the manuscript and supervised the project; PD supervised
611 the project, designed the experiments, and performed the statistical analysis. All authors have read
612 and approved the final version of the manuscript.



613 **References**View Article Online
DOI: 10.1039/D5FO04976H

- 614 1. K. R. Pandey, S. R. Naik and B. V. Vakil, Probiotics, prebiotics and synbiotics- a review, *J Food*
615 *Sci Technol*, 2015, **52**, 7577-7587.
- 616 2. Z. Mujagic, P. De Vos, M. V. Boekschoten, C. Govers, H.-J. H. Pieters, N. J. De Wit, P. A. Bron,
617 A. A. Masclee and F. J. Troost, The effects of *Lactobacillus plantarum* on small intestinal
618 barrier function and mucosal gene transcription; a randomized double-blind placebo
619 controlled trial, *Scientific reports*, 2017, **7**, 40128.
- 620 3. N. Tewari and P. Dey, Navigating Commensal Dysbiosis: Gastrointestinal Host-Pathogen
621 Interplay in Orchestrating Opportunistic Infections, *Microbiological Research*, 2024, 127832.
- 622 4. K. Hodgkinson, F. El Abbar, P. Dobranowski, J. Manoogian, J. Butcher, D. Figeys, D. Mack and
623 A. Stintzi, Butyrate's role in human health and the current progress towards its clinical
624 application to treat gastrointestinal disease, *Clinical Nutrition*, 2023, **42**, 61-75.
- 625 5. J. Chen and L. Vitetta, The Role of Butyrate in Attenuating Pathobiont-Induced
626 Hyperinflammation, *Immune Netw*, 2020, **20**, e15.
- 627 6. N. Recharla, R. Geesala and X. Z. Shi, Gut Microbial Metabolite Butyrate and Its Therapeutic
628 Role in Inflammatory Bowel Disease: A Literature Review, *Nutrients*, 2023, **15**.
- 629 7. T. Zhang, W. Zhang, C. Feng, L.-Y. Kwok, Q. He and Z. Sun, Stronger gut microbiome
630 modulatory effects by postbiotics than probiotics in a mouse colitis model, *npj Science of*
631 *Food*, 2022, **6**, 53.
- 632 8. T. Van de Wiele, P. Van den Abbeele, W. Ossieur, S. Possemiers and M. Marzorati, The
633 simulator of the human intestinal microbial ecosystem (SHIME®), *The Impact of Food*
634 *Bioactives on Health: in vitro and ex vivo models*, 2015, 305-317.
- 635 9. Y. Qi, L. Yu, F. Tian, J. Zhao and Q. Zhai, In vitro models to study human gut-microbiota
636 interactions: Applications, advances, and limitations, *Microbiological Research*, 2023, **270**,
637 127336.
- 638 10. L. Sardelli, S. Perottoni, M. Tunesi, L. Boeri, F. Fusco, P. Petrini, D. Albani and C. Giordano,
639 Technological tools and strategies for culturing human gut microbiota in engineered in vitro
640 models, *Biotechnology and bioengineering*, 2021, **118**, 2886-2905.
- 641 11. S. Renwick, C. M. Ganobis, R. A. Elder, C. Gianetto-Hill, G. Higgins, A. V. Robinson, S. J.
642 Vancuren, J. Wilde and E. Allen-Vercoe, Culturing human gut microbiomes in the laboratory,
643 *Annual Review of Microbiology*, 2021, **75**, 49-69.
- 644 12. X. Zhao, N. B. Gökgöz, Z. Xie, L. M. Jakobsen, D. S. Nielsen and H. C. Bertram, Effects of
645 calcium supplementation on the composition and activity of in vitro simulated gut
646 microbiome during inulin fermentation, *Food & Function*, 2025, **16**, 2857-2869.
- 647 13. C. Liu, W. Jiang, F. Yang, Y. Cheng, Y. Guo, W. Yao, Y. Zhao and H. Qian, The combination of
648 microbiome and metabolome to analyze the cross-cooperation mechanism of *Echinacea*
649 *purpurea* polysaccharide with the gut microbiota in vitro and in vivo, *Food & Function*, 2022,
650 **13**, 10069-10082.
- 651 14. F. Koc, M. Sabuncu, G. G. Yavuz, G. Düven, R. M. K. Abdo, U. Bağci, Y. Şahan, S. Ö. Toğay, R.
652 P. Ross and C. Stanton, Exploring tarhana's prebiotic potential using different flours in an in
653 vitro fermentation model, *Food & Function*, 2025, **16**, 4754-4771.
- 654 15. C. Nicco, A. Paule, P. Konturek and M. Edeas, From Donor to Patient: Collection, Preparation
655 and Cryopreservation of Fecal Samples for Fecal Microbiota Transplantation, *Diseases*, 2020,
656 **8**.
- 657 16. A. L. Goodman, G. Kallstrom, J. J. Faith, A. Reyes, A. Moore, G. Dantas and J. I. Gordon,
658 Extensive personal human gut microbiota culture collections characterized and manipulated
659 in gnotobiotic mice, *Proceedings of the National Academy of Sciences*, 2011, **108**, 6252-6257.
- 660 17. M. Aguirre, J. Ramiro-Garcia, M. E. Koenen and K. Venema, To pool or not to pool? Impact of
661 the use of individual and pooled fecal samples for in vitro fermentation studies, *Journal of*
662 *microbiological methods*, 2014, **107**, 1-7.



- 663 18. K. Newmei, S. Gorai, S. Mukherjee and P. Dey, Nrf2-dependent cytoprotective effects and
 664 depletion of gut microbial energy harvesting by chemically defined polyphenol-rich
 665 *Clerodendrum infortunatum*, *Fitoterapia*, 2025, **185**, 106730. View Article Online
DOI: 10.1039/D5FO04976H
- 666 19. R. Walia, S. R. Chaudhuri and P. Dey, Reciprocal interaction between gut microbiota and
 667 aloe-emodin results in altered microbiome composition and metabolism of aloe-emodin,
 668 *Food Bioscience*, 2025, 107061.
- 669 20. A. Gotoh, M. Nara, Y. Sugiyama, M. Sakanaka, H. Yachi, A. Kitakata, A. Nakagawa, H. Minami,
 670 S. Okuda and T. Katoh, Use of Gifu Anaerobic Medium for culturing 32 dominant species of
 671 human gut microbes and its evaluation based on short-chain fatty acids fermentation
 672 profiles, *Bioscience, biotechnology, and biochemistry*, 2017, **81**, 2009-2017.
- 673 21. X. Teng, T. Zhang and C. Rao, Novel probiotics adsorbing and excreting microplastics in vivo
 674 show potential gut health benefits, *Frontiers in Microbiology*, 2025, **15**, 1522794.
- 675 22. J. Armetta, S. S. Li, T. H. Vaaben, R. Vazquez-Urbe and M. O. Sommer, Metagenome-guided
 676 culturomics for the targeted enrichment of gut microbes, *Nature Communications*, 2025, **16**,
 677 663.
- 678 23. P. Van den Abbeele, C. Grootaert, M. Marzorati, S. Possemiers, W. Verstraete, P. Gérard, S.
 679 Rabot, A. Bruneau, S. El Aidy, M. Derrien, E. Zoetendal, M. Kleerebezem, H. Smidt and T. Van
 680 de Wiele, Microbial community development in a dynamic gut model is reproducible, colon
 681 region specific, and selective for Bacteroidetes and Clostridium cluster IX, *Appl Environ
 682 Microbiol*, 2010, **76**, 5237-5246.
- 683 24. J. Reygner, C. Joly Condette, A. Bruneau, S. Delanaud, L. Rhazi, F. Depeint, L. Abdennebi-
 684 Najar, V. Bach, C. Mayeur and H. Khorsi-Cauet, Changes in composition and function of
 685 human intestinal microbiota exposed to chlorpyrifos in oil as assessed by the SHIME® model,
 686 *International journal of environmental research and public health*, 2016, **13**, 1088.
- 687 25. G. T. Macfarlane, S. Macfarlane and G. Gibson, Validation of a three-stage compound
 688 continuous culture system for investigating the effect of retention time on the ecology and
 689 metabolism of bacteria in the human colon, *Microbial ecology*, 1998, **35**, 180-187.
- 690 26. K. P. Scott, J. C. Martin, S. H. Duncan and H. J. Flint, Prebiotic stimulation of human colonic
 691 butyrate-producing bacteria and bifidobacteria, in vitro, *FEMS Microbiology Ecology*, 2014,
 692 **87**, 30-40.
- 693 27. J. A. Jimenez, T. C. Uwiera, D. W. Abbott, R. R. E. Uwiera and G. D. Inglis, Butyrate
 694 Supplementation at High Concentrations Alters Enteric Bacterial Communities and Reduces
 695 Intestinal Inflammation in Mice Infected with *Citrobacter rodentium*, *mSphere*, 2017, **2**,
 696 10.1128/msphere.00243-00217.
- 697 28. C. Wan, K. Wu, X. Lu, F. Fang, Y. Li, Y. Zhao, S. Li and J. Gao, Integrative analysis of the gut
 698 microbiota and metabolome for in vitro human gut fermentation modeling, *Journal of
 699 Agricultural and Food Chemistry*, 2021, **69**, 15414-15424.
- 700 29. H. Sasaki, H. Masutomi, Y. Kobayashi, K. Toyohara, K. Imaizumi, Y. Nakayama and K. Ishihara,
 701 Evaluation of the Fermentation Characteristics of Prebiotic-Containing Granola and
 702 Short-Chain Fatty Acid Production in an In Vitro Gut Microbiota Model, *Food Science &
 703 Nutrition*, 2025, **13**, e70252.
- 704 30. J. Xia, N. Psychogios, N. Young and D. S. Wishart, MetaboAnalyst: a web server for
 705 metabolomic data analysis and interpretation, *Nucleic Acids Res*, 2009, **37**, W652-660.
- 706 31. P. Dey, G. Y. Sasaki, P. Wei, J. Li, L. Wang, J. Zhu, D. McTigue, Z. Yu and R. S. Bruno, Green tea
 707 extract prevents obesity in male mice by alleviating gut dysbiosis in association with
 708 improved intestinal barrier function that limits endotoxin translocation and adipose
 709 inflammation, *The journal of nutritional biochemistry*, 2019, **67**, 78-89.
- 710 32. X. Sun, P. Dey, R. S. Bruno and J. Zhu, EGCG and catechin relative to green tea extract
 711 differentially modulate the gut microbial metabolome and liver metabolome to prevent
 712 obesity in mice fed a high-fat diet, *The Journal of nutritional biochemistry*, 2022, **109**,
 713 109094.



- 714 33. S. Gandhi, M. R. Saha and P. Dey, Improved antioxidant activities of spice require enrichment
715 of distinct yet closely-related metabolic pathways, *Heliyon*, 2023, **9**, e21392. View Article Online
DOI: 10.1039/D3FO04976H
- 716 34. Z. Pang, J. Chong, G. Zhou, D. A. de Lima Morais, L. Chang, M. Barrette, C. Gauthier, P.
717 Jacques, S. Li and J. Xia, MetaboAnalyst 5.0: narrowing the gap between raw spectra and
718 functional insights, *Nucleic Acids Res*, 2021, **49**, W388-w396.
- 719 35. A. Aiello, F. Pizzolongo, L. De Luca, G. Blaiotta, M. Aponte, F. Addeo and R. Romano,
720 Production of butyric acid by different strains of *Lactobacillus plantarum* (*Lactiplantibacillus*
721 *plantarum*), *International Dairy Journal*, 2023, **140**, 105589.
- 722 36. M. S. Kennedy and E. B. Chang, The microbiome: Composition and locations, *Prog Mol Biol*
723 *Transl Sci*, 2020, **176**, 1-42.
- 724 37. D. Laukens, B. M. Brinkman, J. Raes, M. De Vos and P. Vandenabeele, Heterogeneity of the
725 gut microbiome in mice: guidelines for optimizing experimental design, *FEMS microbiology*
726 *reviews*, 2016, **40**, 117-132.
- 727 38. F. Shanahan, T. S. Ghosh and P. W. O'Toole, Human microbiome variance is underestimated,
728 *Current Opinion in Microbiology*, 2023, **73**, 102288.
- 729 39. P. Dey and S. Ray Chaudhuri, The opportunistic nature of gut commensal microbiota, *Critical*
730 *reviews in microbiology*, 2023, **49**, 739-763.
- 731 40. J. Isenring, L. Bircher, A. Geirnaert and C. Lacroix, In vitro human gut microbiota
732 fermentation models: opportunities, challenges, and pitfalls, *Microbiome Research Reports*,
733 2023, **2**, 2.
- 734 41. T. Shintani, D. Sasaki, Y. Matsuki and A. Kondo, In vitro human colon microbiota culture
735 model for drug research, *Medicine in Drug Discovery*, 2024, **22**, 100184.
- 736 42. S. El Manouni El Hassani, N. K. H. de Boer, F. M. Jansen, M. A. Benninga, A. E. Budding and T.
737 G. J. de Meij, Effect of Daily Intake of *Lactobacillus casei* on Microbial Diversity and Dynamics
738 in a Healthy Pediatric Population, *Curr Microbiol*, 2019, **76**, 1020-1027.
- 739 43. H. Grazul, L. L. Kanda and D. Gondek, Impact of probiotic supplements on microbiome
740 diversity following antibiotic treatment of mice, *Gut Microbes*, 2016, **7**, 101-114.
- 741 44. R. L. Washburn, D. Sandberg and M. A. G. Stofer, Supplementation of a single species
742 probiotic does not affect diversity and composition of the healthy adult gastrointestinal
743 microbiome, *Human Nutrition & Metabolism*, 2022, **28**, 200148.
- 744 45. G. Caballero-Flores, J. M. Pickard and G. Núñez, Microbiota-mediated colonization
745 resistance: mechanisms and regulation, *Nat Rev Microbiol*, 2023, **21**, 347-360.
- 746 46. P. Dey, S. R. Chaudhuri, T. Efferth and S. Pal, The intestinal 3M (microbiota, metabolism,
747 metabolome) zeitgeist—from fundamentals to future challenges, *Free Radical Biology and*
748 *Medicine*, 2021, **176**, 265-285.
- 749 47. H. He, H. Xu, J. Xu, H. Zhao, Q. Lin, Y. Zhou and Y. Nie, Sodium Butyrate Ameliorates Gut
750 Microbiota Dysbiosis in Lupus-Like Mice, *Front Nutr*, 2020, **7**, 604283.
- 751 48. N. W. Smith, P. R. Shorten, E. Altermann, N. C. Roy and W. C. McNabb, The classification and
752 evolution of bacterial cross-feeding, *Frontiers in Ecology and Evolution*, 2019, **7**, 153.
- 753 49. V. R. Marcelino, C. Welsh, C. Diener, E. L. Gulliver, E. L. Rutten, R. B. Young, E. M. Giles, S. M.
754 Gibbons, C. Greening and S. C. Forster, Disease-specific loss of microbial cross-feeding
755 interactions in the human gut, *Nature Communications*, 2023, **14**, 6546.
- 756 50. K. Hou, Z.-X. Wu, X.-Y. Chen, J.-Q. Wang, D. Zhang, C. Xiao, D. Zhu, J. B. Koya, L. Wei and J. Li,
757 Microbiota in health and diseases, *Signal transduction and targeted therapy*, 2022, **7**, 135.
- 758 51. L. Deng and S. Wang, Colonization resistance: the role of gut microbiota in preventing
759 *Salmonella* invasion and infection, *Gut Microbes*, 2024, **16**, 2424914.
- 760 52. P. H. Bradley and K. S. Pollard, Proteobacteria explain significant functional variability in the
761 human gut microbiome, *Microbiome*, 2017, **5**, 1-23.
- 762 53. S. Gupta, A. Fečkaninová, J. Lokesh, J. Koščová, M. Sørensen, J. Fernandes and V. Kiron,
763 *Lactobacillus* Dominate in the Intestine of Atlantic Salmon Fed Dietary Probiotics, *Front*
764 *Microbiol*, 2018, **9**, 3247.



- 765 54. Y. Ji, S. Park, H. Park, E. Hwang, H. Shin, B. Pot and W. H. Holzapfel, Modulation of Active Gut
 766 Microbiota by *Lactobacillus rhamnosus* GG in a Diet Induced Obesity Murine Model, *Front*
 767 *Microbiol*, 2018, **9**, 710. View Article Online
 DOI: 10.1039/D5FO04976H
- 768 55. F. Magne, M. Gotteland, L. Gauthier, A. Zazueta, S. Pesoa, P. Navarrete and R. Balamurugan,
 769 The Firmicutes/Bacteroidetes Ratio: A Relevant Marker of Gut Dysbiosis in Obese Patients?,
 770 *Nutrients*, 2020, **12**.
- 771 56. Y. S. Ji, H. N. Kim, H. J. Park, J. E. Lee, S. Y. Yeo, J. S. Yang, S. Y. Park, H. S. Yoon, G. S. Cho, C.
 772 M. Franz, A. Bomba, H. K. Shin and W. H. Holzapfel, Modulation of the murine microbiome
 773 with a concomitant anti-obesity effect by *Lactobacillus rhamnosus* GG and *Lactobacillus*
 774 *sakei* NR28, *Benef Microbes*, 2012, **3**, 13-22.
- 775 57. V. Singh, G. Lee, H. Son, H. Koh, E. S. Kim, T. Unno and J. H. Shin, Butyrate producers, "The
 776 Sentinel of Gut": Their intestinal significance with and beyond butyrate, and prospective use
 777 as microbial therapeutics, *Front Microbiol*, 2022, **13**, 1103836.
- 778 58. M. E. Salliss, J. D. Maarsingh, C. Garza, P. łaniewski and M. M. Herbst-Kralovetz,
 779 Veillonellaceae family members uniquely alter the cervical metabolic microenvironment in a
 780 human three-dimensional epithelial model, *NPJ Biofilms Microbiomes*, 2021, **7**, 57.
- 781 59. H. M. Wexler, Bacteroides: the good, the bad, and the nitty-gritty, *Clin Microbiol Rev*, 2007,
 782 **20**, 593-621.
- 783 60. C. Bourriaud, R. J. Robins, L. Martin, F. Kozłowski, E. Tenailleau, C. Cherbut and C. Michel,
 784 Lactate is mainly fermented to butyrate by human intestinal microfloras but inter-individual
 785 variation is evident, *J Appl Microbiol*, 2005, **99**, 201-212.
- 786 61. S. Kim, S. H. Chun, Y. H. Cheon, M. Kim, H. O. Kim, H. Lee, S. T. Hong, S. J. Park, M. S. Park, Y.
 787 S. Suh and S. I. Lee, *Peptoniphilus gorbachii* alleviates collagen-induced arthritis in mice by
 788 improving intestinal homeostasis and immune regulation, *Front Immunol*, 2023, **14**,
 789 1286387.
- 790 62. M. Vital, A. C. Howe and J. M. Tiedje, Revealing the bacterial butyrate synthesis pathways by
 791 analyzing (meta)genomic data, *mBio*, 2014, **5**, e00889.
- 792 63. R. B. Canani, M. D. Costanzo, L. Leone, M. Pedata, R. Meli and A. Calignano, Potential
 793 beneficial effects of butyrate in intestinal and extraintestinal diseases, *World J*
 794 *Gastroenterol*, 2011, **17**, 1519-1528.
- 795 64. M. A. Tufail and R. A. Schmitz, Exploring the Probiotic Potential of *Bacteroides* spp. Within
 796 One Health Paradigm, *Probiotics Antimicrob Proteins*, 2025, **17**, 681-704.
- 797 65. P. Amiri, S. A. Hosseini, S. Ghaffari, H. Tutunchi, S. Ghaffari, E. Mosharkesh, S. Asghari and N.
 798 Roshanravan, Role of Butyrate, a Gut Microbiota Derived Metabolite, in Cardiovascular
 799 Diseases: A comprehensive narrative review, *Front Pharmacol*, 2021, **12**, 837509.
- 800 66. E. A. Franzosa, A. Sirota-Madi, J. Avila-Pacheco, N. Fornelos, H. J. Haiser, S. Reinker, T.
 801 Vatanen, A. B. Hall, H. Mallick, L. J. McIver, J. S. Sauk, R. G. Wilson, B. W. Stevens, J. M. Scott,
 802 K. Pierce, A. A. Deik, K. Bullock, F. Imhann, J. A. Porter, A. Zhernakova, J. Fu, R. K. Weersma,
 803 C. Wijmenga, C. B. Clish, H. Vlamakis, C. Huttenhower and R. J. Xavier, Gut microbiome
 804 structure and metabolic activity in inflammatory bowel disease, *Nat Microbiol*, 2019, **4**, 293-
 805 305.
- 806 67. X. Du, Q. Li, Z. Tang, L. Yan, L. Zhang, Q. Zheng, X. Zeng, G. Chen, H. Yue, J. Li, M. Zhao, Y. P.
 807 Han and X. Fu, Alterations of the Gut Microbiome and Fecal Metabolome in Colorectal
 808 Cancer: Implication of Intestinal Metabolism for Tumorigenesis, *Front Physiol*, 2022, **13**,
 809 854545.
- 810 68. F. Candelieri, M. Simone, A. Leonardi, M. Rossi, A. Amaretti and S. Raimondi, Indole and p-
 811 cresol in feces of healthy subjects: Concentration, kinetics, and correlation with microbiome,
 812 *Front Mol Med*, 2022, **2**, 959189.
- 813 69. S. Kishino, M. Takeuchi, S. B. Park, A. Hirata, N. Kitamura, J. Kunisawa, H. Kiyono, R.
 814 Iwamoto, Y. Isobe, M. Arita, H. Arai, K. Ueda, J. Shima, S. Takahashi, K. Yokozeki, S. Shimizu



- 815 and J. Ogawa, Polyunsaturated fatty acid saturation by gut lactic acid bacteria affecting host
 816 lipid composition, *Proc Natl Acad Sci U S A*, 2013, **110**, 17808-17813. View Article Online
DOI: 10.1039/D5FO04976H
- 817 70. Z. Majka, B. Zapala, A. Krawczyk, K. Czamara, J. Mazurkiewicz, E. Stanek, I. Czyzyska-Cichon,
 818 M. Kepczynski, D. Salamon, T. Gosiewski and A. Kaczor, Direct oral and fiber-derived
 819 butyrate supplementation as an anti-obesity treatment via different targets, *Clin Nutr*, 2024,
 820 **43**, 869-880.
- 821 71. C. H. Hu, L. Q. Ren, Y. Zhou and B. C. Ye, Characterization of antimicrobial activity of three
 822 *Lactobacillus plantarum* strains isolated from Chinese traditional dairy food, *Food Sci Nutr*,
 823 2019, **7**, 1997-2005.
- 824 72. H. Cai, Z. Wen, X. Xu, J. Wang, X. Li, K. Meng and P. Yang, Serum Metabolomics Analysis for
 825 Biomarkers of *Lactobacillus plantarum* FRT4 in High-Fat Diet-Induced Obese Mice, *Foods*,
 826 2022, **11**.
- 827 73. D. Parekh, R. Saydjari, J. Ishizuka, C. M. Townsend, Jr. and J. C. Thompson, Sodium butyrate
 828 stimulates polyamine biosynthesis in colon cancer cells, *Surg Oncol*, 1992, **1**, 315-322.
- 829 74. C. orline Nzeteu, F. Coelho, A. C. Trego, F. Abram, J. Ramiro-Garcia, L. Paulo and V.
 830 O'Flaherty, Development of an enhanced chain elongation process for caproic acid
 831 production from waste-derived lactic acid and butyric acid, *Journal of Cleaner Production*,
 832 2022, **338**, 130655.
- 833 75. J. Bassaganya-Riera, M. Viladomiu, M. Pedragosa, C. De Simone, A. Carbo, R. Shaykhutdinov,
 834 C. Jobin, J. C. Arthur, B. A. Corl, H. Vogel, M. Storr and R. Hontecillas, Probiotic bacteria
 835 produce conjugated linoleic acid locally in the gut that targets macrophage PPAR γ to
 836 suppress colitis, *PLoS One*, 2012, **7**, e31238.
- 837 76. N. K. Krishnamoorthy, M. Kalyan, T. A. Hediya, N. Anand, P. H. Kendaganna, G. Pendyala, S.
 838 V. Yelamanchili, J. Yang, S. B. Chidambaram, M. K. Sakharkar and A. M. Mahalakshmi, Role of
 839 the Gut Bacteria-Derived Metabolite Phenylacetylglutamine in Health and Diseases, *ACS*
 840 *Omega*, 2024, **9**, 3164-3172.
- 841 77. A. K. Rana, S. S. Kumar Saraswati, V. Anang, A. Singh, A. Singh, C. Verma and K. Natarajan,
 842 Butyrate induces oxidative burst mediated apoptosis via Glucose-6-Phosphate
 843 Dehydrogenase (G6PDH) in macrophages during mycobacterial infection, *Microbes Infect*,
 844 2024, **26**, 105271.
- 845 78. Q. Luo, N. Ding, Y. Liu, H. Zhang, Y. Fang and L. Yin, Metabolic engineering of microorganisms
 846 to produce pyruvate and derived compounds, *Molecules*, 2023, **28**, 1418.
- 847 79. T. Takeuchi, T. Kubota, Y. Nakanishi, H. Tsugawa, W. Suda, A. T.-J. Kwon, J. Yazaki, K. Ikeda, S.
 848 Nemoto and Y. Mochizuki, Gut microbial carbohydrate metabolism contributes to insulin
 849 resistance, *Nature*, 2023, **621**, 389-395.
- 850 80. A. J. Wolfe, Glycolysis for microbiome generation, *Microbiology spectrum*, 2015, **3**,
 851 10.1128/microbiolspec.mbp-0014-2014.
- 852 81. K. Oliphant and E. Allen-Vercoe, Macronutrient metabolism by the human gut microbiome:
 853 major fermentation by-products and their impact on host health, *Microbiome*, 2019, **7**, 1-15.
- 854 82. F. M. Elshaghabee, W. Bockelmann, D. Meske, M. De Vrese, H.-G. Walte, J. Schrezenmeir and
 855 K. J. Heller, Ethanol production by selected intestinal microorganisms and lactic acid bacteria
 856 growing under different nutritional conditions, *Frontiers in microbiology*, 2016, **7**, 47.
- 857 83. A. Solmonson and R. J. DeBerardinis, Lipoic acid metabolism and mitochondrial redox
 858 regulation, *Journal of Biological Chemistry*, 2018, **293**, 7522-7530.
- 859 84. D. R. Donohoe, N. Garge, X. Zhang, W. Sun, T. M. O'Connell, M. K. Bunger and S. J. Bultman,
 860 The microbiome and butyrate regulate energy metabolism and autophagy in the mammalian
 861 colon, *Cell metabolism*, 2011, **13**, 517-526.
- 862 85. T. van Deuren, E. E. Blaak and E. E. Canfora, Butyrate to combat obesity and
 863 obesity-associated metabolic disorders: Current status and future implications for
 864 therapeutic use, *Obesity Reviews*, 2022, **23**, e13498.



- 865 86. H. Liu, S. Wang, J. Wang, X. Guo, Y. Song, K. Fu, Z. Gao, D. Liu, W. He and L.-L. Yang, Energy metabolism in health and diseases, *Signal transduction and targeted therapy*, 2025, **10**, 69. View Article Online
DOI: 10.1039/D5FO04976H
- 866
- 867 87. G. Den Besten, K. Van Eunen, A. K. Groen, K. Venema, D.-J. Reijngoud and B. M. Bakker, The
- 868 role of short-chain fatty acids in the interplay between diet, gut microbiota, and host energy
- 869 metabolism, *Journal of lipid research*, 2013, **54**, 2325-2340.
- 870 88. M. D. Spalding and S. T. Prigge, Lipoic acid metabolism in microbial pathogens, *Microbiol Mol*
- 871 *Biol Rev*, 2010, **74**, 200-228.
- 872 89. R. Chaudhry and M. Varacallo, *Biochemistry, glycolysis*, 2018.
- 873 90. P. K. Arnold and L. W. S. Finley, Regulation and function of the mammalian tricarboxylic
- 874 acid cycle, *J Biol Chem*, 2023, **299**, 102838.
- 875 91. S. Starke, D. M. Harris, J. Zimmermann, S. Schuchardt, M. Oumari, D. Frank, C. Bang, P.
- 876 Rosenstiel, S. Schreiber and N. Frey, Amino acid auxotrophies in human gut bacteria are
- 877 linked to higher microbiome diversity and long-term stability, *The ISME journal*, 2023, **17**,
- 878 2370-2380.
- 879 92. C. Nie, T. He, W. Zhang, G. Zhang and X. Ma, Branched Chain Amino Acids: Beyond Nutrition
- 880 Metabolism, *Int J Mol Sci*, 2018, **19**.
- 881 93. D. G. Burrin and B. Stoll, Metabolic fate and function of dietary glutamate in the gut, *Am J*
- 882 *Clin Nutr*, 2009, **90**, 850s-856s.
- 883 94. V. L. Albaugh, K. Mukherjee and A. Barbul, Proline precursors and collagen synthesis:
- 884 biochemical challenges of nutrient supplementation and wound healing, *The Journal of*
- 885 *nutrition*, 2017, **147**, 2011-2017.
- 886 95. J. Wang, H. Ji, S. Wang, H. Liu, W. Zhang, D. Zhang and Y. Wang, Probiotic *Lactobacillus*
- 887 *plantarum* promotes intestinal barrier function by strengthening the epithelium and
- 888 modulating gut microbiota, *Frontiers in microbiology*, 2018, **9**, 1953.
- 889 96. Z. Wang, Y. Ohata, Y. Watanabe, Y. Yuan, Y. Yoshii, Y. Kondo, S. Nishizono and T. Chiba,
- 890 Taurine Improves Lipid Metabolism and Increases Resistance to Oxidative Stress, *J Nutr Sci*
- 891 *Vitaminol (Tokyo)*, 2020, **66**, 347-356.
- 892
- 893



894 **Figure legends**

View Article Online
DOI: 10.1039/D5FO04976H

895 **Figure 1:** Brief experimental design of the study. Fecal sample from healthy individual was used as
896 inoculum for gut bacteria and treated with *L. plantarum* (probiotic) and butyrate (post-biotic) in an
897 individual fermenter of AMMR system. After 48 h of treatment, the sample were collected for
898 subsequent metagenomic and metabolomic analyses.

899
900 **Figure 2:** Shifts in microbiome profile in response to butyrate and *L. plantarum* treatments. (A-C)
901 Bar plots representing relative abundance of taxa at (A) phylum, (B) order, and (C) genus levels
902 across the treatments. (D-F) Differential genus identification using STAMP between (D) control v/s
903 butyrate, (E) control v/s *L. plantarum*, and (F) *L. plantarum* v/s butyrate. (G) Correlation heatmap
904 depicting degree of association between identified genera and the treatments

905
906 **Figure 3:** Functional metagenomic predictions using PICRUSt. Differential prediction of KEGG
907 orthologs (KO) in (A) control v/s butyrate and (B) control v/s *L. plantarum*. (C) Common predicted
908 KO across the treatments. (D) Heatmap showing the relative abundance of KO among the different
909 treatments

910
911 **Figure 4:** Metabolomic profiling of gut microbes under the influence of butyrate and *L. plantarum*
912 treatments. (A) Representative GC-MS graph for all treatments with retention time (min) on x-axis
913 and intensity on y-axis. (B) Venn diagram showing common metabolites identified across the
914 treatments. (C-E) STAMP plots showing the differential abundant metabolites between (C) control
915 v/s butyrate, (D) control v/s *L. plantarum*, and (E) butyrate v/s *L. plantarum*. (F) Correlation heatmap
916 depicting the degree of association between identified metabolites with the treatments. (G) Venn
917 diagram representing the metabolite class common across the treatments. (H-J) Metabolite class
918 enrichment in (H) control, (I) butyrate, and (J) *L. plantarum* treatments. The x-axis represents
919 enrichment ratio value and y-axis depicts the significance value of enrichment.

920



921 **Figure 5:** Metabolic pathway enrichment in (A) control, (B) butyrate, and (C) *L. plantarum*. The x-
922 axis corresponds to pathway impact value and y-axis depicts significance of impact value. 1.
923 Riboflavin metabolism, 2. D-amino acid metabolism, 3. Pyrimidine metabolism, 4. Phenylalanine,
924 tyrosine and tryptophan biosynthesis, 5. Phenylalanine metabolism, 6. Lipoic acid metabolism, 7.
925 Galactose metabolism, 8. Pyruvate metabolism, 9. Tryptophan metabolism, 10. Purine metabolism,
926 11. Other carbon fixation pathways, 12. One carbon pool by folate, 13. Propanoate metabolism, 14.
927 Pentose phosphate pathway, 15. Glycolysis or gluconeogenesis, 16. Fatty acid degradation, 17.
928 Fatty acid biosynthesis, 18. Arginine and proline metabolism, 19. Biosynthesis of unsaturated fatty
929 acids, 20. Valine, leucine and isoleucine degradation, 21. Taurine and hypotaurine metabolism, 22.
930 Lysine degradation, 23. Valine, leucine and isoleucine biosynthesis, 24. Methane metabolism, 25.
931 Sulfur metabolism, 26. Alanine, aspartate and glutamate metabolism, 27. Glyoxylate and
932 dicarboxylate metabolism, 28. Selenocompound metabolism, 29. Arginine biosynthesis, 30. Glycine,
933 serine and threonine metabolism, 31. Lysine biosynthesis. (D) Venn diagram representing the
934 pathway common across the treatments.



Figure 1

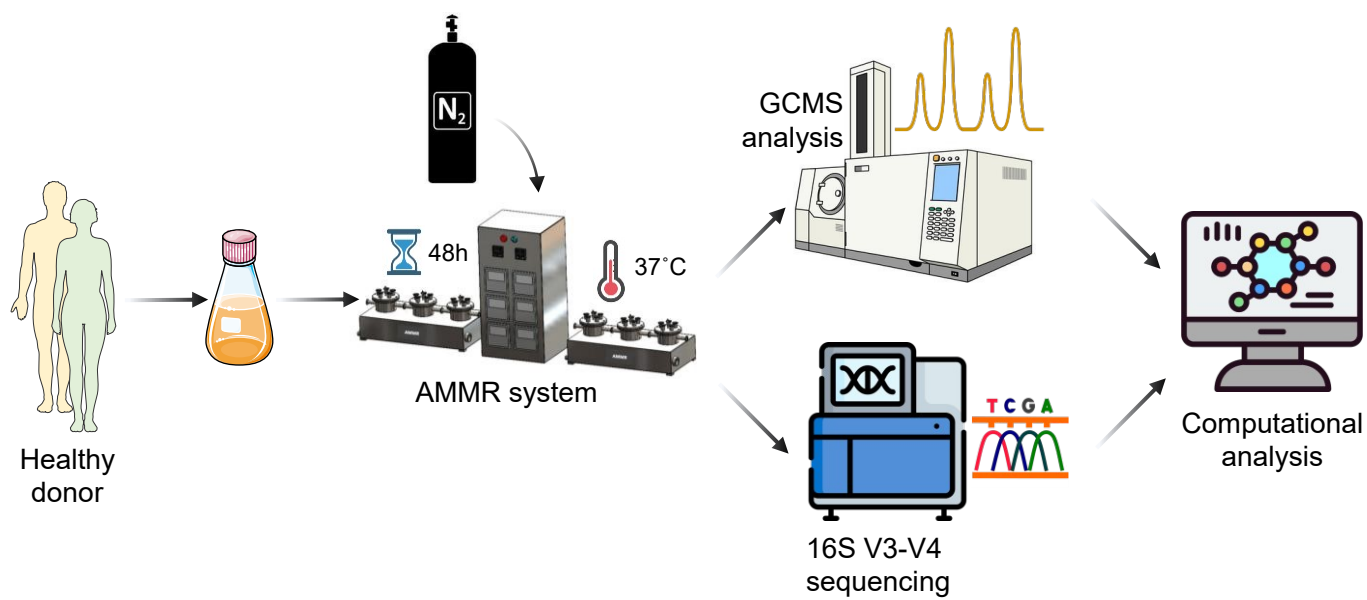
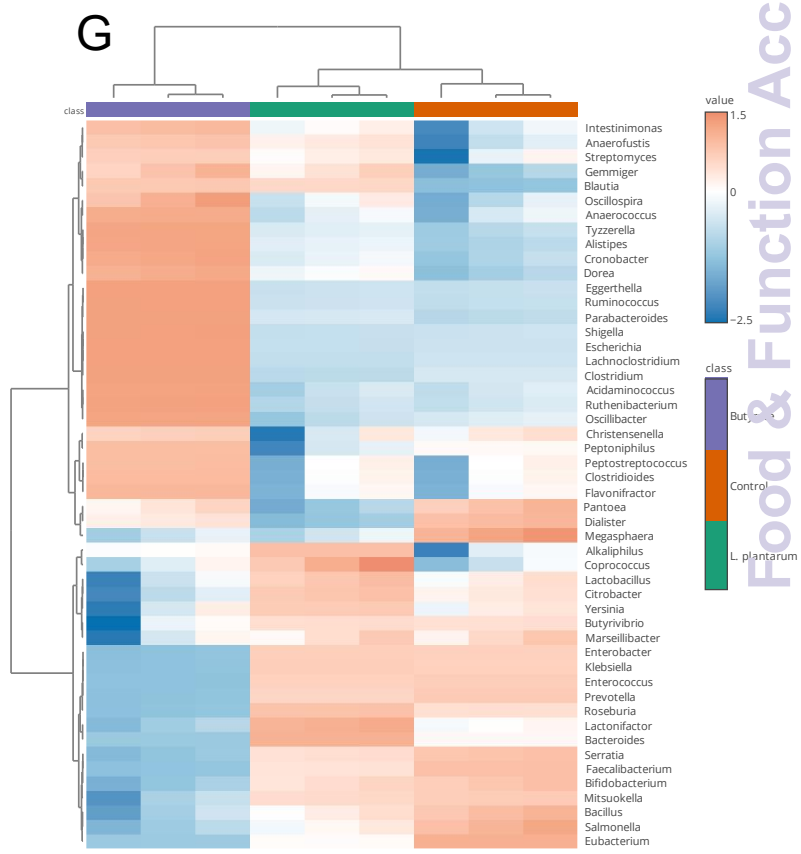
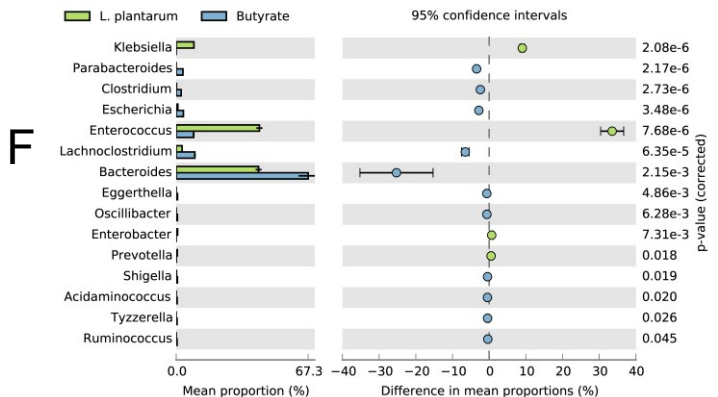
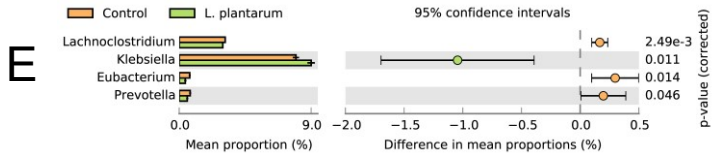
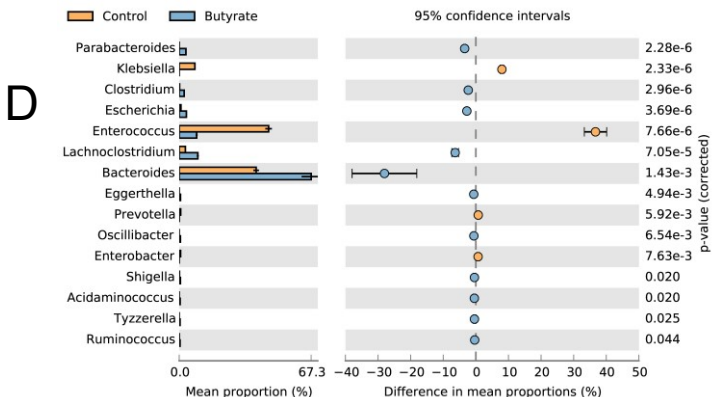
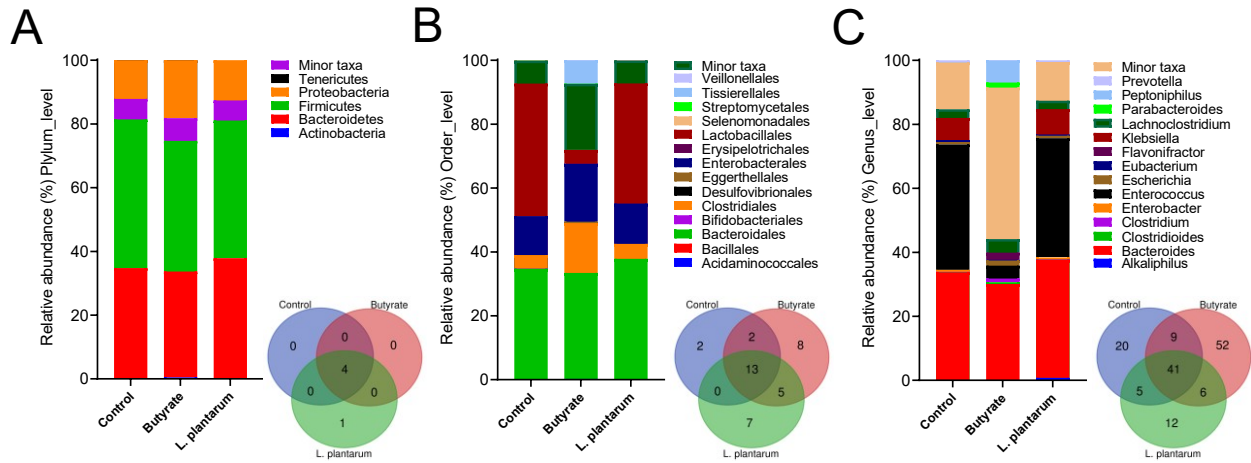


Figure 2



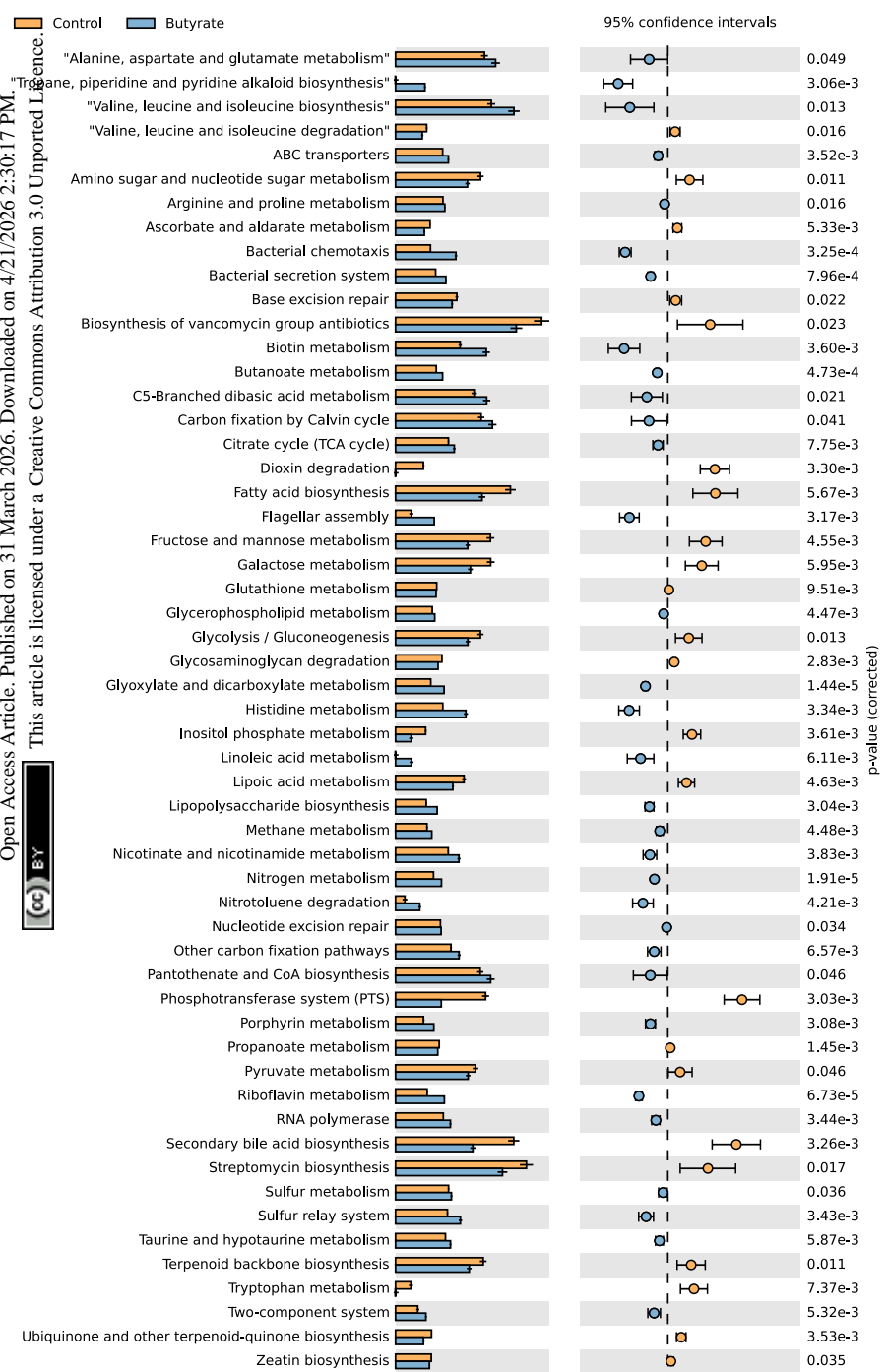
Food & Function Accepted Manuscript

Open Access Article. Published on 31 March 2026. Downloaded on 4/21/2026 2:30:17 PM. This article is licensed under a Creative Commons Attribution 3.0 Unported Licence.

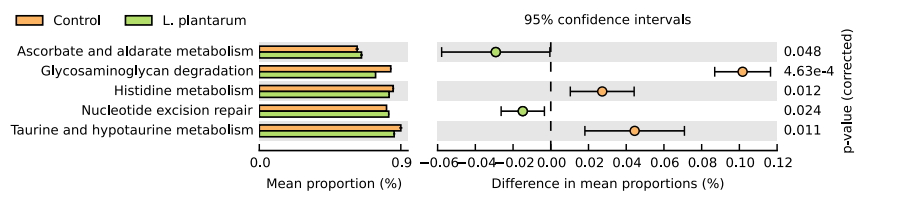


abundance (%)
View Article Online
DOI: 10.1039/D5FO00493H

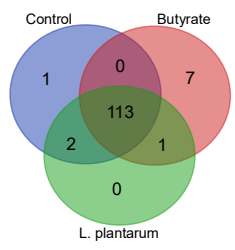
A



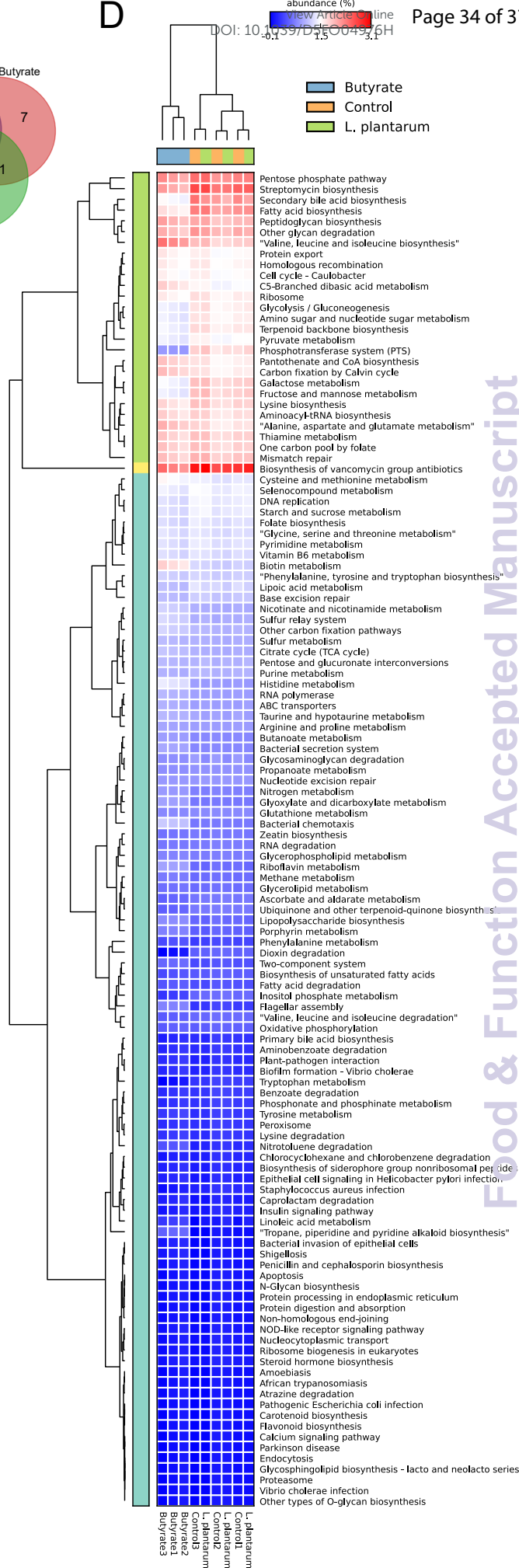
B



C



D

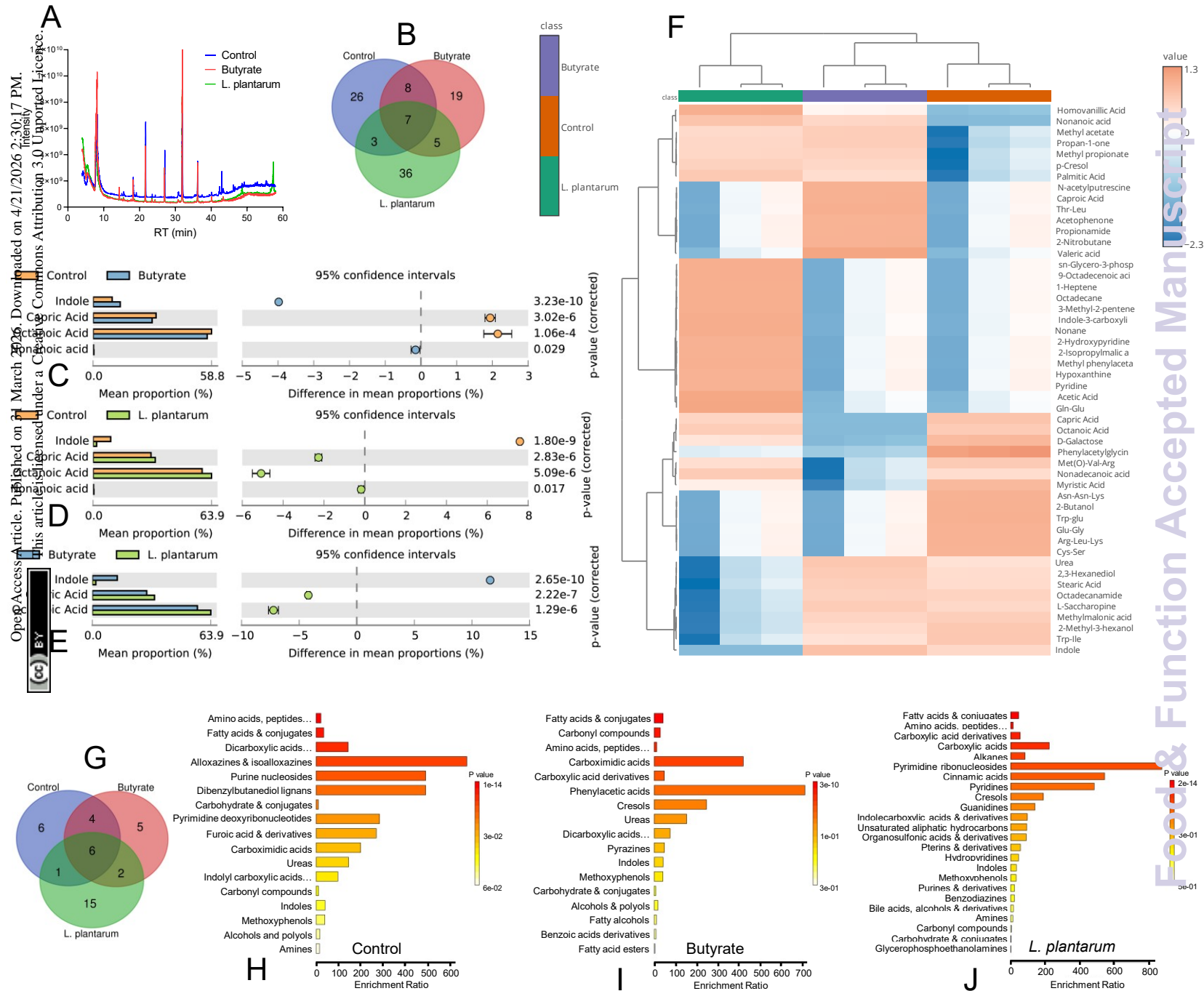


Food & Function Accepted Manuscript

Open Access Article. Published on 31 March 2026. Downloaded on 4/21/2026 2:30:17 PM. This article is licensed under a Creative Commons Attribution 3.0 Unported Licence.



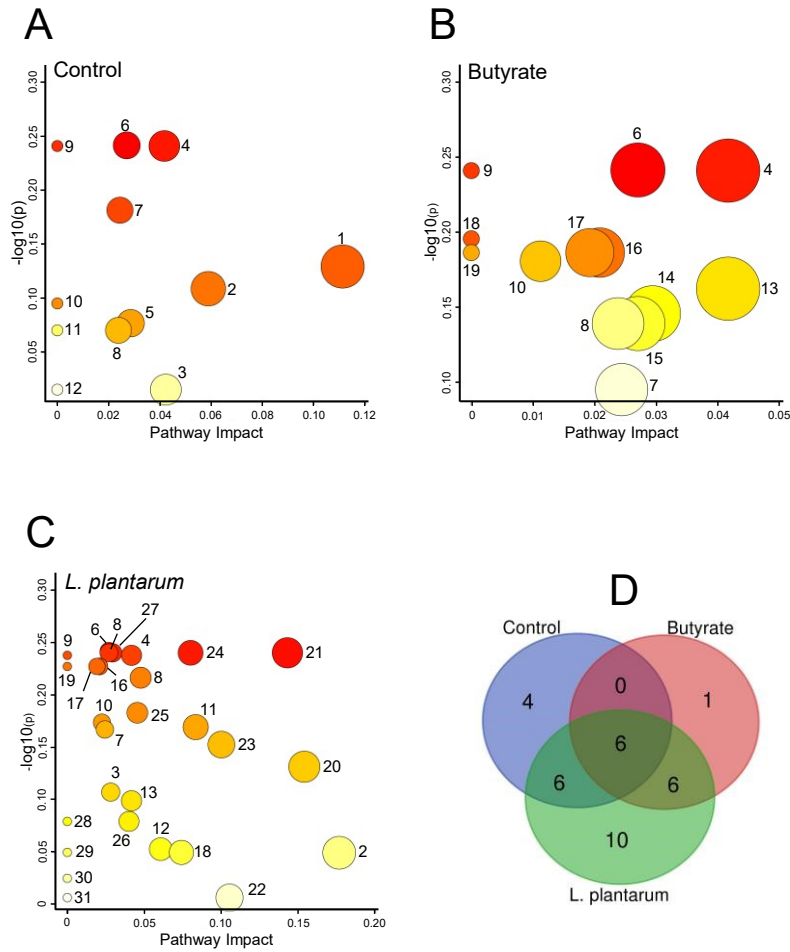
Figure 4



Open Access Article. Published on 07 March 2025. Downloaded on 4/21/2026 2:30:17 PM.
This article is licensed under a Creative Commons Attribution 3.0 Unported Licence.

Food & Function Accepted Manuscript

Figure 5



All necessary data are included in the supplementary information.

View Article Online
DOI: 10.1039/D5FO04976H



Open Access Article. Published on 31 March 2026. Downloaded on 4/21/2026 2:30:17 PM.
This article is licensed under a Creative Commons Attribution 3.0 Unported Licence.